THE REPUBLIC OF TURKEY
İSTANBUL KÜLTÜR UNIVERSITY
INSTITUTE OF GRADUATE STUDIES

INFLUENCE OF THE SOIL AMPLIFICATION ON THE SEISMIC RESPONSE OF BASE ISOLATED STRUCTURES

MASTER OF SCIENCE THESIS

HAMDULLAH ATIED

Department: Civil Engineering

Program: Structural Engineering

Supervisor: Assist. Prof. Dr. Gökhan YAZICI

August 2022

THE REPUBLIC OF TURKEY
İSTANBUL KÜLTÜR UNIVERSITY
INSTITUTE OF GRADUATE STUDIES

THE INFLUENCE OF THE SOIL AMPLIFICATION ON THE SEISMIC RESPONSE OF BASE ISOLATED STRUCTURES

M.Sc. Thesis

HAMDULLAH ATIED

1700004766

Date of submission: 6/09/2022

Date of defense examination: 19/09/2022

Supervisor and Chairperson: **Assist. Prof. Dr. Gökhan YAZICI**

Members of Examining Committee: **Prof. Dr. Necmettin GÜNDÜZ**

Assist. Prof. Dr. Erdal COŞKUN

My dissertation is dedicated to my parents and family, who have always been a constant source of inspiration and support and have taught me to work hard to pursue my dreams.

ACKNOWLEDGEMENT

Firstly, I would like to express my thanks to my patient and supportive supervisor, Assist. Prof. Dr. Gökhan YAZICI, for their invaluable contribution and insightful feedback.

I shall also express my gratitude to respectful jury members for their valuable time and extreme patience.

Finally, I would like to thank Istanbul Kultur University for providing me with the opportunity to be a part of such a great university and for fostering such a positive learning environment. I would also like to thank the academic and administrative staff for their dedication throughout these difficult times and for helping us in this journey.

Hamdullah Atied

TABLE OF CONTENTS

LIST OF ABBREVIATION

NEHRP	National Earthquake Hazards Reduction Program
FEMA	Federal Emergency Management Agency
PEER	Pacific Earthquake Engineering Research Centre
THA	Time History Analysis
NTHA	Nonlinear Time History Analysis
LRB	Lead Rubber Bearing
HDRB	High Damping Rubber Bearing
FPS	Friction Pendulum Sliding
SRA	Site Response Analysis
UBC	Uniform Building Code
SA	Soil Amplification
SSI	Soil-Structure Interaction
PGA	Peak Ground Acceleration
PGV	Peak Ground velocity
PGD	Peak Ground Displacement
MATLAB	Matrix Laboratory

LIST OF TABLES

LIST OF FIGURES

LIST OF SYMBOLS

β	Damping ratio
b	Short plan dimension
d	Total diameter of plate
M_s	Mass of structure
M_b	Base mass
C	Damping ratio
K	Stiffness
H	Story height
D_d	Design displacement
e	Eccentricity
W_d	Dissipated energy
g	Acceleration of gravity
G	Shear modulus of rubber
C_v	Seismic coefficient
F_a	Site coefficients
S_{ae}	Spectral acceleration
S_d, S_m	Design, and maximum spectral acceleration
ÿ$_g$	Ground motion acceleration
ÿ$_t$	Total acceleration
ẏ	Relative velocity
u	Relative displacement
ω	Natural frequency
ω_s, ω_b	Superstructure and base mass Natural frequency
ϒ	Mass ratio
T_d	Time period

K_{eff}	Effective stiffness
W	Weight of structure
β_{eff}	Effective damping ratio
Q	Characteristic strength of isolation
K_1	Elastic stiffness
K_2	Post elastic stiffness
D_y	Yield displacement
F_y	Initial yield force
T_r	Total thickness of LRB
α	Strain reduction factor
M	Magnitude of earthquake
β_{eff}	Effective shear strain
V_s	Shear modulus
ρ	Density of the soil
τ	Stress-strain relationship
G_0	Maximum shear modulus
♈	Shear strain
♈$_r$	Reference shear strain
S	Dimensionless exponent
a, b	Are fitting curve parameters
σ_v	Vertical overburden effective stress to the soil layers
σ_{ref}	Reference confining pressure
c, d	Fitting curve parameters
F_n	Natural frequency of the relevant mode and n is the mode number
F_{bb}(♈)	Backbone curve

Üniversite : **İstanbul Kültür Üniversitesi**

Enstitü : **Lisansüstü Eğitim Enstitüsü**

Anabilim Dalı : **Inşaat Mühendisliği**

Programı : **Yapı**

Tez Danışmanı : **Dr. Öğretim Üyesi Gökhan YAZICI**

ÖZET

Bu çalışma, sismik yalıtımlı bir yapının sismik tepkisi üzerindeki yerel zemin koşullarına bağlı zemin büyütmesinin etkisini araştırmaktadır. Zemin büyütme etkileri, DEEPSOIL ile doğrusal tek boyutlu saha tepkisi analizi kullanılarak değerlendirilmştir. Bu araştırmada kullanılan yapısal model, kurşun çekirdekli elastomer mesnetler üzerinde bir kayma çerçevesidir. Kurşun çekirdekli elastomer mesnetlerin kuvvet-yer değiştirme ilişkisi Bouc-Wen modeli ile modellenmiştir. Yapısal modelin dinamik analizi, bir Matlab betiği kullanılarak yapılmıştır. Sismik yalıtımlı yapı modelinin sismik davranışı, altı deprem kuvvetli yer hareketi kaydı ile zaman tanım alanında incelenmiştir. Seçilen deprem yer hareketlerine doğrudan maruz kalan yapının dinamik tepkisi ile zemin tepki analizinden elde edilen serbest yüzey yer hareketlerine maruz kalan yapının dinamik tepkisinin karşılaştırılması, yerel zemin koşullarının yapıların dinamik tepkisini önemli ölçüde değiştirebileceğini göstermektedir.

Anahtar Kelimeler: Zemin Büyütmesi, Sismik izolasyon, Kurşun çekirdekli elastomer mesnetler, MATLAB, DEEPSOIL, Doğrusal olmayan zaman geçmişi analizi

University : **İstanbul Kültür University**

Institute : **Institute of Graduate Studies**

Department : **Civil Engineering**

Program : **Structural Engineering**

Supervisor : **Assist. Prof. Dr. Gökhan YAZICI**

ABSTRACT

This study investigates the influence of soil amplification due to local site conditions on the seismic response of a base-isolated structure. Soil amplification effects were evaluated using linear one-dimensional site response analysis with DEEPSOIL. The structural model used in this investigation is a shear frame on lead core rubber bearings. The force-displacement relationship of the lead core rubber bearings was modeled with the Bouc-Wen model. The dynamic analysis of the structural model was conducted using a MATLAB script. The seismic response of the base-isolated structural model was investigated using time history analysis with six earthquake-strong ground motion records. A comparison of the dynamic response of the structure directly subjected to the selected earthquake ground motions and the free surface ground motions obtained from site response analysis shows that local site conditions can significantly change the dynamic response of structures.

Keywords: soil amplification, seismic isolation, LRB type isolation, MATLAB, DEEPSOIL, Non-linear time history analysis

CHAPTER I

INTRODUCTION

Earthquake causes lateral forces to be applied to the structure, and structural engineers should consider it during the design process. One of the most critical and complex topics facing structural engineers is the seismic design of structures [1]. The goal of seismic design is to increase structural resistance to earthquakes. It situates earthquake structural engineering within a framework of demand and supply equilibrium. The structural response is examined and evaluated using a framework of three quantities: stiffness, strength, and ductility, which correspond to the three critical serviceability limit states [2]. This three-parameter strategy also aligns well with the secondary goals of saving time, lowering repair costs, and safeguarding lives. Various novel technologies have been developed to decrease seismic energy, and base isolation is one of them.

Base isolation is a promising solution for seismic protection of structures in earthquake-prone areas [3]. The base isolation concept has created a breakthrough in a new era of earthquake-resistant building construction. The main idea of base isolation is to separate the superstructure from its base. The base isolation system can be used in new construction and retrofit applications. This technology may be applied to various structures, including schools, hospitals, and multi-story buildings. Installing a base isolation system requires the structure to be free to move horizontally relative to the ground motions. The isolators can be installed at the basement column's top, bottom, or mid-height. The primary goal of base isolation is the protection of the structure and its contents from seismic activities, and structures with base isolators are more predictable and hence have a higher level of reliability than conventional

structures. However, base isolation is less efficient for high-rise buildings and soft soils and requires highly skilled engineers for design and implementation [4].

It is well known that passing through low impedance surficial layers increases the amplitude of seismic waves as they reach the earth's surface. When evaluating ground motion parameters for seismic design of structures, the impact of local soil conditions is taken into consideration. Soil amplification that causes structural damage is one of the most significant effects on the ground surface caused by strong ground motion [5]. Dynamic analyses carried out in accordance with analytical techniques based on specific site conditions can be used to assess soil amplification, as can investigations based on the outcomes of in-situ testing techniques. Since ground motion properties are evaluated for the seismic design of structures, the effects of local site conditions are taken into account. Based on these, the design spectrum is developed, the stresses and dynamic deformations for the evaluation of liquefaction hazards are evaluated, and the earthquake-induced stresses that could lead to structures are evaluated. Site response analysis is used to predict the effects caused in a soil deposit due to seismic loads. The first places where the soil effect seemed to have a noticeable impact on structural response were nuclear power facilities [6].

The primary ground excitation risk is surface rupture, which can result from either vertical or horizontal movement. Structures may sustain significant damage due to ground displacement affecting huge land areas. Understanding the dynamic properties of rock and soil under earthquake or vibration conditions and how to handle seismic problems are the main goals of geotechnical earthquake engineering. This study aims to understand better the linear behavior of soil, which can be used to define different response parameters for the ground response problems, including displacement, velocity, and acceleration to the input motion parameters. The base-isolated structure system separates the superstructure from the foundation or substructure as a means of earthquake protection. The amount of energy that is delivered to the superstructure during an earthquake is greatly decreased by separating the building from its base.

1.1 LITERATURE REVIEW

Garevski et al. researched how the base isolation system combined with soil affects the reaction of multi-story frames during ground motions, as mentioned in Eurocode 8, part1. Soil is classified as dense, moderately dense, and loose soil. Non-linear dynamic analysis was used to examine the effects of soil on structural behavior. The dynamic analysis was carried out using ANSYS, a general finite element tool that allows for modeling of both soil and structure.

One of the advantages of adopting base isolation in the structure is decreasing the structure's response during an earthquake. The analytical investigation's findings indicate that the modeling of the soil layer is essential for the base-isolated structures, especially in soft soil [7].

Aden et al. investigated the seismic analysis of a reinforced concrete (RC) frame with soil effects. To analyze the soil effect in frame structures with base isolation systems, the spring stiffness approach was used to simulate the soil's reaction to the EL Centro ground motion and analyzed with SAP2000 software.

They found that the effect of base isolation and soil on the behavior of a building subjected to seismic loading is widely accepted. The outcome of the analytical investigation shows that modeling soil is important for the base-isolated structures, especially in soft soil. [8].

Alavi & Alidoost researched the impacts of soil on isolated structures built on a variety of soil types to assess the integrated system's seismic reactions quantitatively and qualitatively. A lumped mass with equal spring stiffness and damper is used to represent the superstructure above the isolator in the model. The fixed and soil base-isolated models are subjected to dynamic response spectrum analysis.

SA's impact on the seismic response of the isolated structure can be considerable depending mainly on the soil type, the stiffness and the mass of the superstructure, the aspect ratio of the building, and the foundation properties. The soil effect increases the fundamental periods of the base-isolated structures on the different soil types and with different heights [9].

Abdoulaye Sall et al. work to highlight the soil effects with a linear alternation of the mechanical characteristics of the soil with depth.

This research shows that if the subgrade's elastic modulus is considered constant in the soil mass, the linearity leads to higher displacements. Furthermore, the soil's poisons ratio and the concrete's mechanical qualities do not affect displacements. This paper also reveals that the model's parameter is particularly sensitive to spots in the upper soil's half thickness [10].

Yin's study aims to understand better the non-linear liquefied soil behaviors, the base-isolated structure system, and their interactions during earthquake ground motions.

The eigenvalue analysis of the system matrix reveals that the soil extends the structure periods. It is obvious to see the relationship between the system reactions and the hysteretic frictional force. Among isolators, the base isolation system with a strong hysteretic frictional force performs less effectively. This means that determining the impact of shear wave velocity on soil stiffness is more challenging[11].

Eduardo et al. investigated soil's effect on the dynamic response of isolated base mid-rise buildings. A discrete shear building model with a flexible foundation, and linear elastic elastomeric bearing, is studied using an appropriate approach for systems with nonclassical damping. The model is used to assess whether seismic isolation in soft soil is practicable.

They found that the isolated base structure could be employed to effectively manage the negative soil impacts expected for these buildings positioned at sites with fundamental periods longer than the superstructure of fixed base natural period [12].

Sayyad & Bhusare conducted the research to assess available literature on soil, base isolation, and the implicit of both on structure performance. Furthermore, it investigates the structure with and without considering the interaction between the soil and the building and finally studies the performance of a base-isolated structure while considering the soil effect. The NTHA and RSA are used for earthquake response.

When soil is addressed on an isolated structure, the time period of the structure increases, and the soil affects reaction quantities such as displacements, acceleration, and base shear. When soil behavior is considered in the study, the responses of the base-isolated structure are enhanced. Soil should be considered for base-isolated buildings, especially when established on soft soil because soil deformation at the

isolation level is greatly influenced. In soft and medium soils with base isolation, the effect of soil is particularly noticeable [13].

Karabork et al. proposed that the influence of soil on the response of isolated buildings was explored in this paper. They studied the dynamic behavior of multi-story buildings on soft soil using HDRB response base isolation systems. Different models were created with and without considering soil's effect. Linear models were used for both the soil and the superstructure. The SAP2000 computer software was used to examine the behavior of the required models under dynamic loads.

The findings suggest that in choosing a suitable isolator for base-isolated buildings on soft soil, the soil is an essential factor to consider in terms of earthquakes. When the soil effect is not considered, the system efficiency is inversely proportional to the lateral isolator stiffness. When it comes to soil efficiency, however, the stiffness of the isolator is directly proportional to the efficiency. The selection of suitable isolators should be made with care, considering both fixed support and soil considerations[14].

Sravya1 & Manchalwar investigated the impact of soil and the effects of a U-shaped steel damper on the building's base isolated response. For three distinct soil conditions, the structure was studied utilizing five floors with an isolated basis with soil and an isolated base without soil effect, which were analyzed using time history analysis in SAP2000 software. An isolated base building's seismic performance under four different ground motions was examined in this investigation.

Using steel damper-shaped and soil compact decreased structural reactions. Considering the soil effect on the structure adds some flexibility to the structure by increasing the displacements of the building. As a result, better structural response prediction can be achieved by modeling base isolation and considering soil [15].

Bandyopadhyay et al. the influence of soil between two reinforced concrete (RC) three-story structures supported with base isolator type LRB while the other is a standard RC framed structure located in India's highest seismic zone is investigated in this research. For modeling and analysis using finite element software, NTHA was used for the dynamic response of both structures.

They founds that the base-isolated structure had a frequency that was 2.6 times lower than the conventional structure, and the response was also lowered by a factor of 4 to 5 as expected; however, in the reaction of the base-isolated building, SA was seen, and the measured response revealed the frequency of the surrounding structure. It's also been discovered that when PGA increases, the frequency of the isolated building decreases [16].

Hassan & Pal1 conducted this paper to investigate soil condition's effect below the base-isolated, and NTHA and RSA were performed using ETABS-2015 software. The impact of soil elasticity is considered in this study to examine the differences in spectral acceleration, base shear, story displacement, story drift, and story shear produced using Indian standard seismic code provisions. several soils are thoroughly studied and handled for the seismic performance of multi-story structures.

They found that as soil flexibility and superstructure stiffness rise, the value of base shear increases. It was also founded that spectral acceleration and displacement are more significant in soft soil conditions, implying that a structure's response spectrum is connected to soil conditions. A report indicates that hard and medium soils are suitable for base isolation construction [17].

Even though there has been some advancement in this area, the earthquake tragedy continues to cause significant loss of life and damage to property. This work aims to understand better soil's linear behavior and the effect of soil amplification on base-isolated structures. A collection of six near-fault seismic ground motions will be used in parametric research to check the effect of soil on the SDOF base-isolated structure. This study is designed into six chapters, which are as bellows:

- Chapter one introduces soil amplification and base isolation system, literature review, the objective, and thesis organization.
- Chapter two gives an overview of the base isolation system and types of isolation.
- Chapter three illustrates the design parameter of LRB isolation and numerical modeling of LRB in MATLAB software with considering six ground motion data.

- Chapter four overviews soil amplification and SRA, a one-dimensional SRA of soil with the description and numerical study of soil amplification in DEEPSOIL software.
- Chapter five presents the result and discussion of the effect of soil on base-isolated structure, and the acceleration data will be taken from the DEEPSOIL analysis result and show how it interacts on the structure.
- Chapter six, the last chapter of the research, presents the conclusion, reference, and appendix.

CHAPTER II

BASE ISOLATION

2.1 Overview

The most common loads that demand lateral design of a structure are wind and earthquake [18]. Earthquake load is uncontrollable and designing a structure to withstand a very large seismic demand is impractical. The most common approach to dealing with seismic demand is to increase the ductility of the building or the elastic strength of the structure. Engineers must enhance the capacity to exceed the demand. Instead of boosting capacity, base isolation uses the opposite technique of reducing seismic demand [19].

A method for improving the seismic performance of structures such as buildings and bridges is seismic isolation [20]. The technology was first proposed at the end of the 19th century. Seismic isolation is currently a well-established technology that is gaining popularity and is used all over the world.

The concept of isolation is to separate the structure from ground excitation by using a flexible or sliding interface. The structure can sway dramatically during an earthquake if the ground shaking frequency is near the building's natural frequency. The seismic energy is mitigated and dissipated by the base isolation system [21]. Therefore, base isolation protects structural integrity by reducing structural displacement. In other words, the base isolators allow the building to move over the ground with less frequency [18].

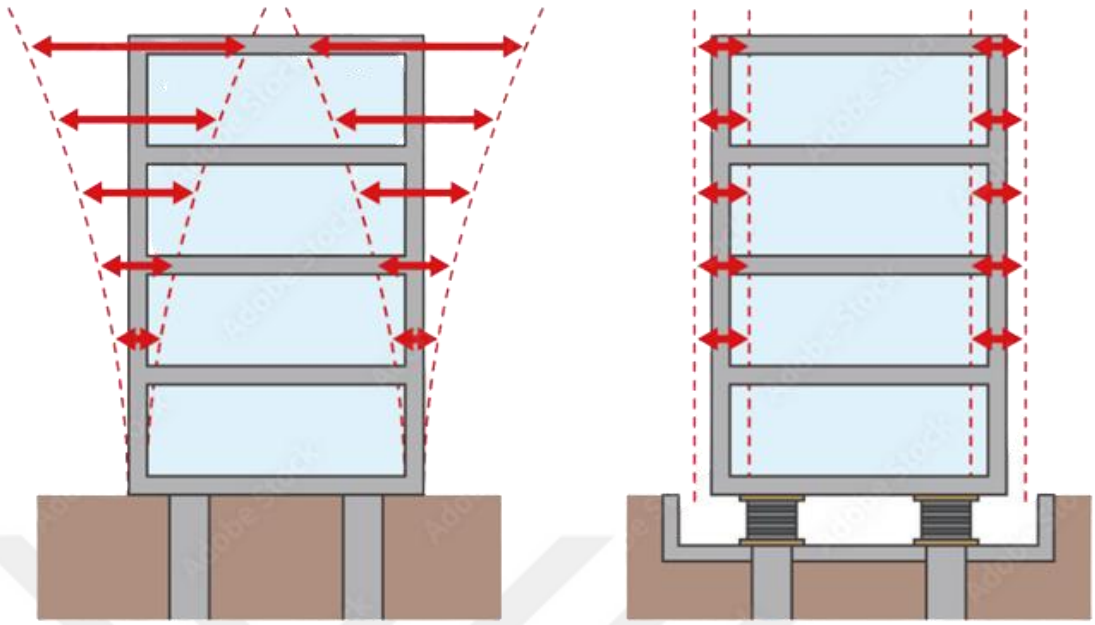

Figure 2.1 Effect of Base Isolation [22]

The following are the basic dynamic impacts of base isolation on the superstructure:

- Increasing the structure's natural period
- Decreasing the acceleration responses and inter-story displacement

The fundamental frequency is reduced in base-isolated buildings, and the first vibration mode is apart from the others. As a result, the superstructure can be supposed to remain linear, and any possible damages can be initiated at the base level. Base isolation extends the natural period, and total building displacement to total height and inter-story drift compared to normal foundations [23].

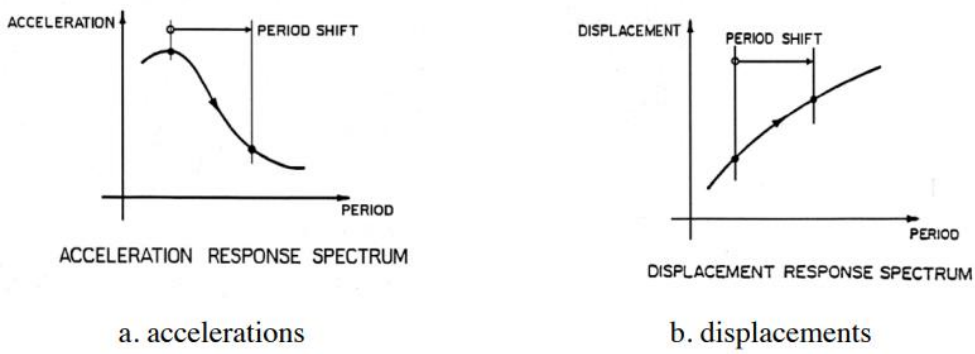

a. accelerations b. displacements

Figure 2.2 Effect of Seismic Period Elongation on Structure [24]

The points which need more attention in base isolation systems are [25].

- Base isolation structure evaluation and approval guidelines.
- Facilities to promote the gathering, and sharing, of technical knowledge on the response of the structure.
- Research into methods for evaluating response control structure performance.

2.2 Types of Base Isolation Devices

For improving the earthquake resistance of a building, structural engineers may use two categories of isolation systems: elastomeric bearings and sliding isolation bearings.

2.2.1 Elastomeric Bearings

Elastomeric bearings are made up of layers of steel and rubber. The lead rubber bearing (LRB) and the high damping rubber bearing (HDRB) are widely used types of elastomeric isolators. In 1969, civil engineers in Skopje Republic of Macedonia employed unreinforced rubber bearings for the first time to protect an elementary school [26].

Lead Rubber Bearings (LRB)

For many years, engineers preferred to use the LRB type of frequent isolation devices, which link isolation and energy dissipation in an individual small unit. The building is separated from the horizontal components of the earthquake's ground excitation in this method. The main purpose of the LRB isolator is to increase the frame structure's lateral flexibility, which allows ground accelerations to be passed into the superstructure to be reduced considerably. These LRB isolator devices produce vertical load support, horizontal flexibility, and additional damping to protect the structure against seismic loads. The LRB isolator is built up of a laminated rubber elastomeric bearing, steel shim plates, cover plates, and a lead core in the center, as shown in Figure 3.

The LRB has the advantage of being a single combined stiffness at service load levels, flexibility at seismic load levels, and damping. Because of these characteristics, LRB is one of the most popular types of isolators utilized where significant amounts of damping are required, such as in high seismic zones or where structural integrity is crucial under service loads like bridges. The LRB is employed in this study, and it was developed by William Robinson in New Zealand [27].

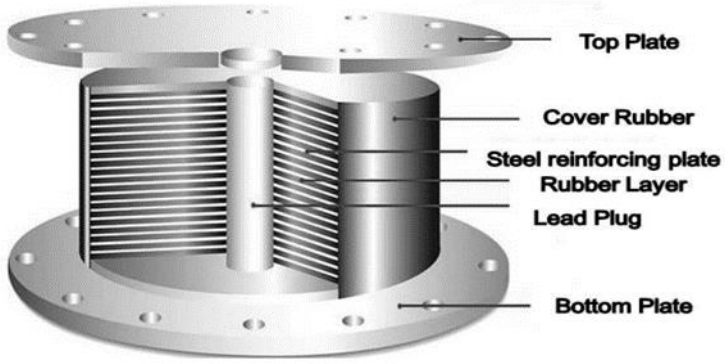

Figure 2.3 Lead Rubber Bearing (LRB) [22]

High Damping Rubber Bearings (HDRB)

HDRB is made up of an alternate course of rubber and steel plates linked together by vulcanization, as illustrated in Figure 4.

The rubber compound in HDRB has high damping properties. HDRB is relatively stiff for small strains and flexible for large strains. This characteristic is advantageous because it permits the structure to respond rigidly to low excitation such as wind while allowing for large flexibility excitations such as earthquakes.

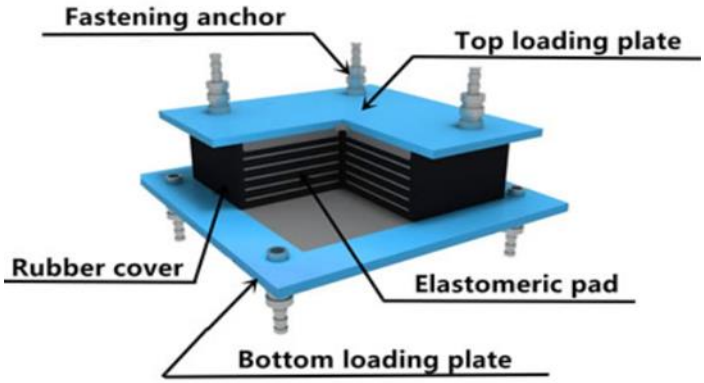

Figure 2.4 High Damping Rubber Bearing (HDRB) [23]

2.2.2 Sliding Isolators

These isolators work on the friction principle and prevent shear from being transferred over the isolation interface. Consider two plates that can slide over each other the sliding only begins when the earthquake's exciting force exceeds the frictional force between the plates.

Friction Pendulum Sliding (FPS) Bearing:

The FPS was matured by providing a round sliding interface to adjust for the target isolation period while friction between the sliding interfaces supports energy dissipation. Therefore, when it comes to lengthening a structure's fundamental period, the FPS is functionally equal to the HDRB and LRB, with the added benefits of period invariance, temperature insensitivity, and durability. Because its qualities are relatively unaffected by aging or temperature, the FPS has recently gained popularity [28,29]. These bearings have been used in a variety of structures such as buildings, bridges, and industrial facilities.

Single Pendulum Bearing:

The original friction pendulum bearing is the single pendulum bearing. The vertical load support is maintained in the center of the structural components by a single slider.

(a) Single Pendulum bearing cross section (b) Single pendulum motion maximum credible earthquake

Figure 2.5 Single Friction Pendulum Sliding Bearing [22]

Triple Pendulum Bearing:

The triple pendulum bearing combines three pendulums into a single bearing, each with attributes chosen to improve the structures' reaction to various earthquake strengths and frequencies. Figure 6 shows the various lateral movement stages of a triple pendulum bearing.

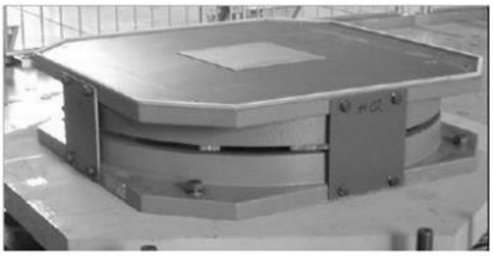

(a) 3D view of Triple Pendulum Bearing

(b) Different stages of vibration of Triple Pendulum Bearing

Figure 2.6 Triple Pendulum Bearing [22]

2.3 Advantages of Base Isolation Systems

- The structure's seismic demand is lowered, resulting in lower construction costs.
- During an earthquake, there is less structural displacement.
- Improv structural safety.
- Reduced the amount of damage caused by an earthquake.
- Improve the structural performance under earthquake loads.
- Property preservation.

Base isolation appears to be a very promising solution for seismic excitation protection in various structures. Engineers discovered the need to maintain the superstructure stable when seismic activities are shaking the substructure. As a result, base isolation is the optimum strategy because it avoids a significant amount of destruction and has a low maintenance cost. The base isolation concept has created a new era in earthquake-resistant building construction, and it will prove to be a lifesaving innovation as time goes on.

CHAPTER III

LRB Isolator Design Procedures

3.1 Numerical Modelling

This section explains how to model a LRB base isolation, and data of the isolated system is taken from Bandyopadhyay et al. [16]. The best method of protecting a structure against earthquake effects is base isolation. The idea behind such a system relies on installing bearings to decouple the building from the lateral force of earth motions [31]. The main elements of the structures did not bend during the seismic excitations because these bearings removed the seismic forces. The LRB is the most extensively used elastomeric bearing system when compared to other isolation systems because it has a simple preliminary design process and low initial and ongoing maintenance costs. Due to all these profits, in this research LRB was used.

As shown in Figure 7, an LRB bearing has fixed steel surfaces at the top and bottom, numerous sequenced thin layers, and a lead core in the center of the rubber. LRB is a type of base isolation that makes use of significant damping.

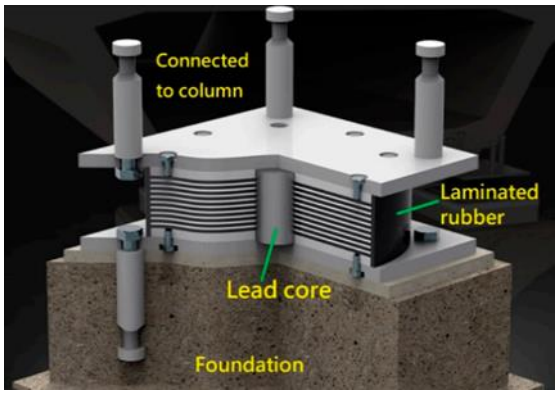

Figure 3.1 Explanation of Lead Rubber Bearing [22]

Steel is rigid under service loads and provides vertical stiffness to isolation systems. The lead core dissipates energy and prevents excessive displacement under

heavy lateral stresses [32]. The lead plug is forced into the elastomeric bearings to create the required tight fit by making the lead plug slightly larger than the hole. Lead plug rubber isolators are used together with low damping natural rubber bearings to achieve the needed superstructure response. The performance of buildings separated with these bearings was shown to be good during certain significant earthquakes. One of the most recent examples was the 1991 isolation of the USC university by a lead rubber bearing. The hospital was unaffected by the 1994 northbridge earthquake and continued to operate.

The LRB combines the functions of vertical support, stiffness at service load levels, and horizontal flexibility at earthquake stress to provide an economical solution to seismic isolation challenges. The mechanical properties of lead are continually restored by the simultaneous interrelated processes of recovery, recrystallization, and grain growth when it is plastically deformed at environment temperature, a process known as the hot working of lead. At plastic strains, lead has good fatigue characteristics while cycling. The lead plug hole can be machined into the bearing after it has been constructed or drilled into the steel and rubber sheets before they are combined. The lead must fit firmly in the elastomeric bearing, which is accomplished by making the lead plug slightly (1%) larger than the hole and forcing it in [32].

Bouc in 1971 [33] introduced the bilinear model, often known as the smoothed bilinear model, which Wen [34] updated in 1976 and called the Bouc-Wen model. This analytical model can be used to analyze a wide variety of hysteretic systems, and it has been confirmed for base isolation of a six-story reinforced concrete building using both elastomeric and sliding isolators by Nagarajaiah et al. [30]. Three factors, elastic stiffness, the ratio of post-yield stiffness, and the yield force, are used to describe the hysteresis model, as shown in Figure 8. Unlike the sharp bilinear model, a circular yield surface function smooths the initial and post-yield stiffness transition, and the two lateral degrees of freedom are connected. The model can thus capture the non-linear properties of isolators under biaxial lateral excitation.

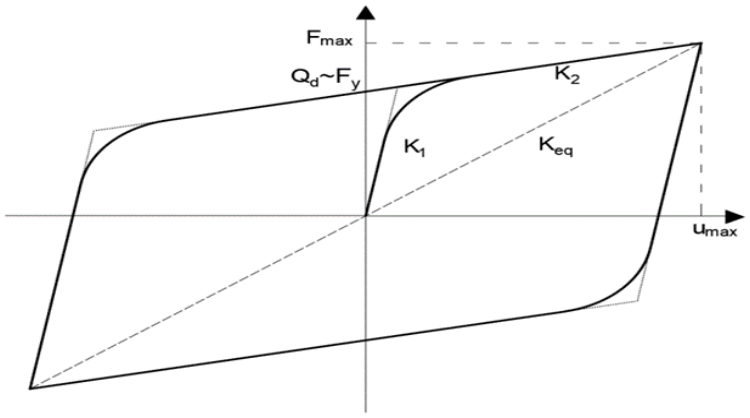

Figure 3.2 Hysteretic Behaviour of LRB Isolator [16]

Figure 9 displays a base isolator schematic diagram and Table 1 shows the lead rubber isolator specifications and design parameters.

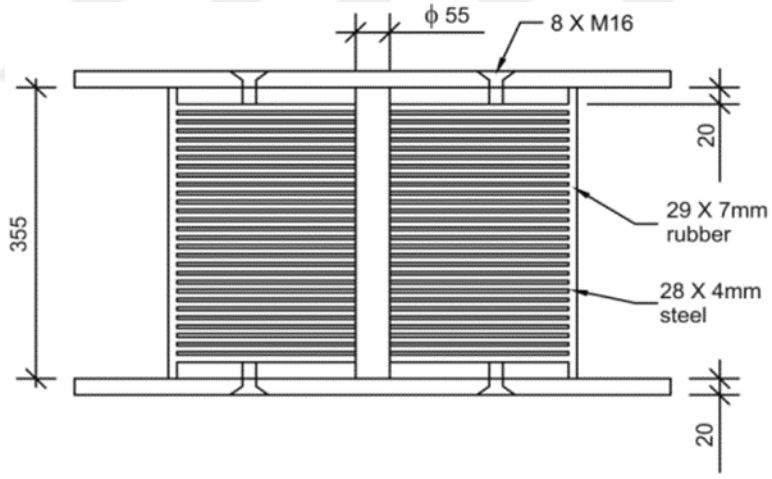

Figure 3.3 Schematic Diagram of LRB Isolator [16]

Design displacement, the isolation system must be designed and built to withstand minimal lateral seismic displacement as estimated by the formula [35]:

$$Dd = \frac{\left(\frac{g}{4\pi^2}\right) * Cv * Td}{\beta d} \qquad (3.1)$$

Where C_v, T_d, and β_d, stand for seismic coefficient, time period, and damping ratio, respectively.

The effective stiffness of an isolator must be calculated for each cycle of stress using the formula [36]:

$$Keff = \frac{W}{g} * (\frac{2\pi}{Td})\text{^}2 \quad (3.2)$$

Where W is the weight of the structure on the isolator

Energy dissipated during the cyclic response of the isolation system:

$$W_d = 2\pi * Keff * Dd^2 * \beta eff \quad (3.3)$$

Where βeff is an effective damping ratio

The below formula calculates the characteristic strength of isolation:

$$Q = \frac{Wd}{4Dd} \quad (3.4)$$

The shape of the force modification curve of LRB applied to cyclic loading is a bilinear curve with an elastic stiffness (K_1), and a post elastic stiffness (K_2) is calculated using the formulas below [35]:

$$K_2 = Keff - \frac{Q}{Dd} \quad (3.5)$$

The value of the multiplier constant to acquire K_1 is estimated from the experiment utilizing a linear expression between initial stiffness K_1 and post-yield stiffness K_2, and it represents in equation (3.6) as 8.7 [16]:

$$K_1 = 8.7*K2 \quad (3.6)$$

Yield displacement is calculated using the eq. (3.7) [35]:

$$D_y = \frac{Q}{K1-K2} \quad (3.7)$$

The initial yield force of LRB is evaluated using eq. (3.8) [35]:

$$F_y = Q+K_2*D_y \quad (3.8)$$

The total thickness of LRB is calculated as per eq. (3.9) [35]:

$$T_r = \frac{Dd}{\gamma'} \tag{3.9}$$

Table 3.1 Design Parameter of LRB Isolator

Parameters	Values
Shim size (mm)	460
Shear modulus of rubber G (mpa)	0.8
Diameter of Lead core (mm)	55
Design displacement (mm)	260
Damping ratio (%)	10
Effective stiffness (KN/m)	11469.27
Dissipated energy (KN)	225.2
Characteristic strength (KN)	216.54
Post yield stiffness (KN/m)	10636.43
Initial stiffness (KN/m)	106364.3
Yield displacement (m)	0.0022
Yield force (KN)	239.94
Maximum shear strain (%)	150

CHAPTER 1V

Site Response Analysis (SRA)

4.1 Overview

The magnitude of the ground excitation, the distance from the epicenter, the duration of ground shaking, the geological environment, the wave propagated through, the frequency content, and the local soil conditions are the variables that affect a site. Site effect has grown to be a major issue for geotechnical seismic engineering within all of these parameters. As a result of seismic waves propagating through soil layers, it changes the motion's characteristics, which has a substantial impact on how structures respond to earthquake events. [36].

The impact of earthquakes on humans and the environment are the focus of geotechnical earthquake engineering. As a result, engineering geologists and geotechnical earthquake engineers seek the most effective strategies for lowering the magnitude of earthquake-related dangers. Determining ground reaction is one of the most important difficulties in geotechnical seismic analysis. Ground response analyses are used to forecast surface ground excitation to produce design response spectra, evaluate dynamic stresses and strains, assess liquefaction hazards, and determine the seismic-applied forces that can cause the instability of the earth and earth retaining structure [37]. Even though seismic waves move tens of kilometers through rock but just a few hundred meters through the soil, the soil significantly impacts the character of ground excitations [37].

Geotechnical earthquake engineers have been attempting to develop methodologies for analyzing ground behavior under earthquake loads that are both practical and acceptable. Understanding the site response of geological materials under seismic loading is required for the creation of a well-established constitutive model. Any seismic soil structure investigation usually starts with an SRA. The goal of this chapter is to give a comprehensive review of SRA.

4.2 The Purpose of SRA

SRA's main objective is to assess how surface-free field ground excitation is impacted by local site factors, underlying soil layer material properties, and surface topographies like cliffs and ridges. Additionally, SRA is a requirement for SA analysis, which must compute the free field site response analysis [37,38].

4.3 The Nature of SRA

The characteristic of site response was studied early, such as Kanai (1952) [39]; it was well understood that the features of the underlying soil deposit affect the surface free field acceleration on the occurrence of ground acceleration. Some frequencies in the input motion are increased as earthquake waves travel upwards through the soil profile and end up in new peaks in the outer layer acceleration response spectrum. The frequencies related to the resonant frequencies of the soil deposit for modest ground excitation create minimal soil strains and, consequently, virtually linear site response. In order to properly assess the seismic risk at a location, a realistic estimate of these amplifications is necessary. The propagation of seismic motions from the base rock, through the overlying soil course, and to the ground's outer surface is assessed using SRA. Response of local soil conditions gives outer surface acceleration time history, surface acceleration response spectra, and spectral amplification factors. The one-dimensional ground response analysis method is highly flexible and can be applied easily to estimate site amplification against ground excitations among the various approaches used for modeling and analyzing site effects.

4.4 One Dimensional Method of SRA

The majority of SRAs used a one-dimensional technique. The result of region soil conditions on ground acceleration wave propagation is evaluated using a one-dimensional response analysis based on the assumptions listed below.

- The profile of soil is made up of horizontal layers piled on top of one another.
- In the horizontal plane, soil layers are homogenous.

- Vertically propagation shear waves are the ground motion that strikes the soil deposit.

These assumptions help to understand the site response phenomenon and enable numerical research using simplified numerical models. Multi-dimensional approaches must be used to assess soil deposits that do not comply with these assumptions.

For many civil engineering applications, the one-dimensional technique is regarded as reasonable and is currently the most often utilized in practice [37]. Body waves propagate away from the source in all directions when a fault ruptures beneath the earth's surface. They are refracted and reflected as they cross the boundaries between different geologic materials. As a result of the fact that shallower materials frequently propagate waves more slowly than deeper ones, inclined rays that hit the boundary of horizontal layers are typically reflected in a more vertical orientation. All boundaries are assumed to be horizontal in one-dimensional ground response calculations, and SH-waves that are propagating vertically from the underlying bedrock are primarily responsible for the reaction of a soil deposit. For one-dimensional ground response analysis, the soil and bedrock surface is assumed to extend infinitely in the horizontal direction.

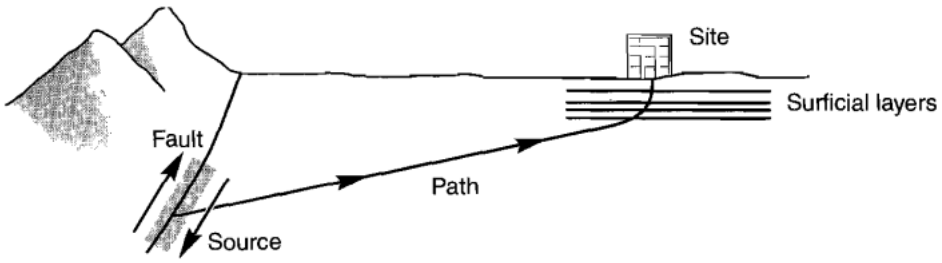

Figure 4.1 Refraction Mechanism Resulting in Vertical Wave Propagation [37]

It is necessary to describe a few concepts that are frequently used to describe ground motions before going on to discuss any of the ground reaction models. Free surface motion is the movement that occurs at a soil deposit surface. A bedrock motion is a movement at the bottom of the soil deposit, and a rock outcropping motion happens when the bedrock is exposed to the surface of the ground.

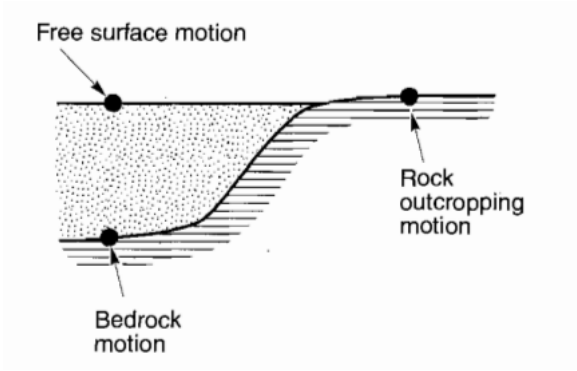

Figure 4.2 Ground Motion Soil Classification Over Bedrock [37]

4.5 Evolution of One-Dimensional SRA Method

In the early site response investigation, the ground acceleration amplification from the bedrock to the soil surface was computed using linear one-dimensional models [40,41].

Since the 1920s, a variety of methodologies for SRA have been developed. Among these are the linear analysis technique in the frequency and time domains, the equivalent linear analysis method in the frequency domain which is total stress analysis, and the non-linear analysis method in the time domain. A non-linear analysis is strain-dependent, whereas linear and equivalent linear studies are based on the independence of the damping and shear modulus from shear strain.

4.6 Linear Approach

Transfer functions are also the foundation for a significant class of methods used in SRA. Transfer functions can be used to define different response parameters for the ground response problems, including displacement, velocity, acceleration, shear stress, and shear strain, to input motion parameters like bedrock acceleration. This method can only be used to analyze linear systems because it is based on the superposition principle. A Fourier series depicts the motion of rocks input over time. The transfer function is then multiplied by each term in the Fourier series of the bedrock input motion to create the Fourier series of the ground surface output motion. The inverse FFT can then be used to depict the mobility of the ground surface output in time. As a result, the transfer function determines whether the soil deposit amplifies or de-amplifies each frequency in the bedrock input motion [37].

4.7 Transfer Function Evaluation

Evaluation of transfer functions is the essential step in the linear approach. Transfer functions are calculated in the following sections for several progressively more complex geotechnical circumstances. Even though the simplest of these may only occasionally apply to actual issues, they highlight some of the significant effects of soil deposits on ground motion characteristics without adding excessive mathematical complexity. The more complicated is frequently employed in geotechnical earthquake engineering practice and can define the most crucial elements of ground response [37].

4.7.1 Homogenous Undamped Soil on Rigid Rock

Firstly, consider a stiff bedrock layer covered in a uniform layer of isotropic, linear elastic soil, as seen in Figure 12. The bedrock harmonic horizontal motion will create vertically propagating shear waves in the soil above.

$$u(z,t) = Ae^{i(\omega t+kz)} + Be^{i(\omega t-kz)} \quad (4.1)$$

Where *A* and *B* are the amplitudes of waves moving in the (-*z*) upward and (+*z*) downward directions, respectively.

For the strain compatibility equation, the solution to the one-dimensional wave equation is:

$$\tau(z,t) = G\,\gamma = G\,\frac{\partial u}{\partial z} \quad (4.2)$$

The strain compatibility to the wave equation will be combined by substituting (4.1) into (4.2) and differentiating the yields:

$$\tau = \mathrm{G}[\mathrm{ik}Ae^{i(\omega t+kz)} - ikBe^{i(\omega t-kz)}] \quad (4.3)$$

The shear strain and shear stress must be (*z=0*) at the free surface, that is:

$$\tau = 0 = \mathrm{Gik}(\mathrm{A}-\mathrm{B})e^{i(\omega t)} \quad (4.4)$$

Where *A=B* , the displacement can be stated as:

$$u(z,t) = 2A\left(\frac{e^{ikz}+e^{-ikz}}{2}\right)e^{i(\omega t)} = 2A\cos(kz)e^{i(\omega t)} \qquad (4.5)$$

With an amplitude of [*2A cos(kz)*] and a fixed shape with respect to depth, the standing wave is created by the constructive interface of the upward and downward traveling waves. A transfer function that describes the ratio of displacement amplitude at any two points in the soil layer can be defined using equation (4.6). The transfer function is determined by selecting these two positions as the top and bottom of the soil layer.

$$F(\omega) = \frac{u_{max}(0,t)}{u_{max}(H,t)} = \frac{2A\cos(0)e^{i(\omega t)}}{2A\cos(\mathrm{KH})e^{i(\omega t)}} = \frac{1}{\cos(KH)} = \frac{1}{\cos\left(\frac{\omega H}{Vs}\right)} \qquad (4.6)$$

It shows that the surface displacement is almost always more than the bedrock displacement and, in some cases, significantly greater due to the denominator can never be bigger than one.

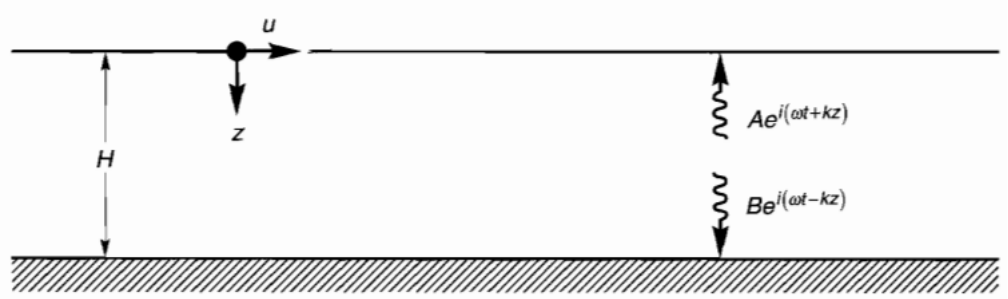

Figure 4.3 Linear Elastic Soil Rest on Top of Stiff Bedrock [37]

The denominator of equation (4.6) approaches $\omega H/V_s$ approaches $n\,\pi$, suggesting that infinite amplification, or resonance, will occur, as shown in Figure 13. Even this very basic model shows how the frequency of the base motion dramatically affects the response of a soil deposit and how the thickness and material properties of the soil layer determine the frequencies at which considerable amplification occurs.

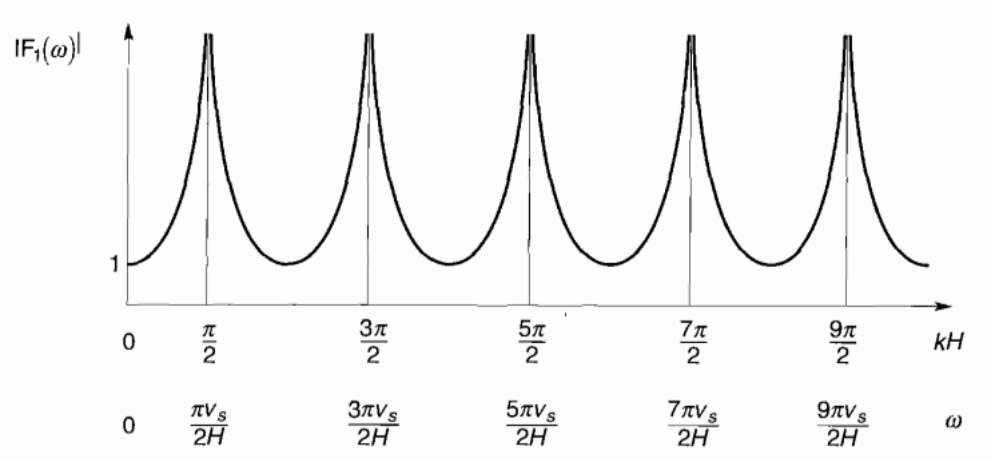

Figure 4.4 Effect of Frequency on the Undamped Linear Elastic Layer [37]

4.7.2 Homogenous damped soil on rigid rock

The previous type assumed that there was no energy loss or damping in the soil. Repeating the analysis using damping will yield more accurate findings because damping exists in all materials.

For strain compatibility use:

$$\tau(z,t) = G\,\gamma + n\,\dot{\gamma} \tag{4.7}$$

For the One-dimensional wave equation:

$$\rho\frac{\partial^2 u}{\partial t^2} = G\frac{\partial^2 u}{\partial z^2} + n\frac{\partial^2 u}{\partial z^2 \partial t} \tag{4.8}$$

The solution for the wave equation is:

$$u(z,t) = Ae^{i(\omega t + k^* z)} + Be^{i(\omega t - k^* z)} \tag{4.9}$$

The complex shear wave velocity can be expressed as:

$$Vs^* = \sqrt{\frac{G^*}{\rho}} = \sqrt{\frac{G(1+i2\xi)}{\rho}} = \sqrt{\frac{G}{\rho}}(1+i\xi) = V_s(1+i\xi) \tag{4.10}$$

$$k^* = \frac{\omega}{Vs^*} = \frac{\omega}{V_s(1+i\xi)} \approx \frac{\omega}{V_s}(1-i\xi) = k(1-i\xi) \tag{4.11}$$

where k^* is a complex wave number

the transfer function for the case of damped soil on hard rock can be written by repeating the prior algebraic operation with the complex wave number.

The amplification function is defined as:

$$F(\omega) = \frac{1}{\cos(k^*H)} = \frac{1}{\cos\left[k(1-\xi)H\right]} = \frac{1}{\sqrt{cos^2(KH)+sinH^2(\xi KH)}} \qquad (4.12)$$

The amplification function can be simplified to $sinH^2$ for small *y*:

$$F(\omega) = \frac{1}{cos^2(k^*H)+(\xi KH)^2} \qquad (4.13)$$

$$F(\omega) = \frac{1}{\sqrt{cos^2\left(\frac{\omega H}{Vs}\right)+\left(\frac{\xi KH}{Vs}\right)}} \qquad (4.14)$$

Equation 4.13 shows that amplification by a damped soil layer also varies with frequency for small damping ratios. The amplification will reach a local maximum whenever $KH = \pi/2 + n\,\pi$, but it will never move to infinity because, for $\xi > 0$, the denominator will always be bigger than zero. Figure 14 displays the fluctuation of the amplification factor with frequency for various damping levels. Figure 13 and Figure 14 comparison demonstrate that damping significantly impacts the response at high frequencies more than at lower frequencies.

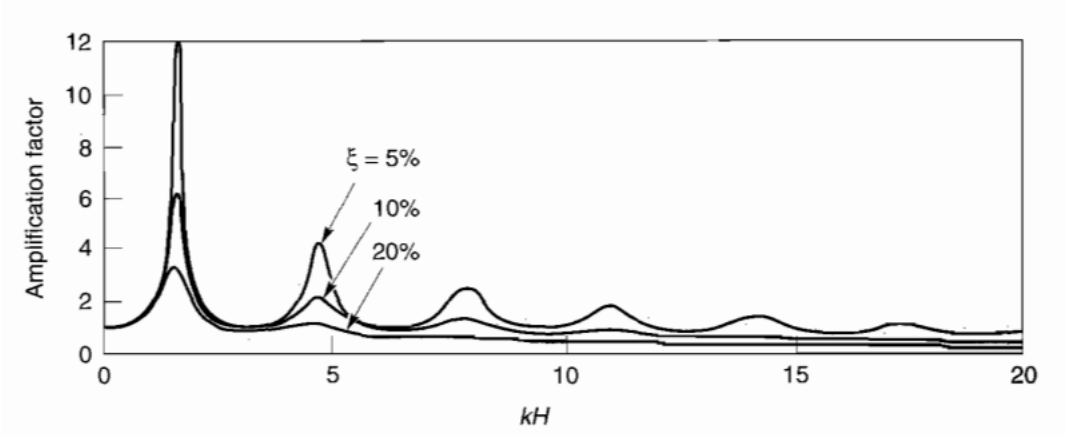

Figure 4.5 Effect of Frequency on The Linear Elastic Damped Layer [37]

The maximum amplification factor will occur about at the lowest natural frequency because the peak amplification factor declines with increasing natural frequency:

$$\omega_0 = \frac{\pi \mathrm{Vs}}{2H} = \frac{2\pi}{Ts} \tag{4.15}$$

The period of vibration corresponding to the fundamental frequency is called the characteristic site period:

$$Ts = \frac{4H}{Vs} \tag{4.16}$$

The characteristic site period gives a beneficial indicator of the period of vibration at which the most significant amplification may be anticipated and depends on the soil's thickness and shear wave velocity.

4.7.3 Homogenous damped soil on elastic rock

If the bedrock is stiff, its motion will not be impacted by changes in the surrounding soil or even the presence of soil. It serves as a rigid end limit, and the stiff layer will reflect any downward-moving waves in the soil back toward the ground surface, retaining all the elastic wave energy within the soil layer. However, if the rock is elastic, downward moving stress waves will only be partially reflected when they reach the soil rock boundary, part of their energy the boundary to continue traveling through the rock.

The elastic energy of these waves will effectively be extracted from the soil layer if the rock extends to a significant depth. This type of radiation damping results in lesser free surface motion amplitude than in the case of rigid bedrock.

$$u_s(z_s, t) = A_s e^{i(\omega t + {k_s}^* z_s)} + B_s e^{i(\omega t - {k_s}^* z_s)} \tag{4.17}$$

$$u_r(z_r, t) = A_r e^{i(\omega t + {k_r}^* z_r)} + B_r e^{i(\omega t - {k_r}^* z_r)} \tag{4.18}$$

As before that, $A_s = B_s$ is the compatibility of displacement and continuity of stresses at the soil rock interface.

$$u_s(z_s = t) = u_r(z_r = 0) \tag{4.19}$$

And τs:

$$\tau_s(z_s = H) = \tau_r(z_r = 0) \tag{4.20}$$

Substituting equations (4.17) into equation (4.18) yields:

$$A_s(e^{i(k_s{}^* H)} + e^{-i(k_s{}^* H)}) = iG_r k_r{}^*(A_r - B_r) \tag{4.21}$$

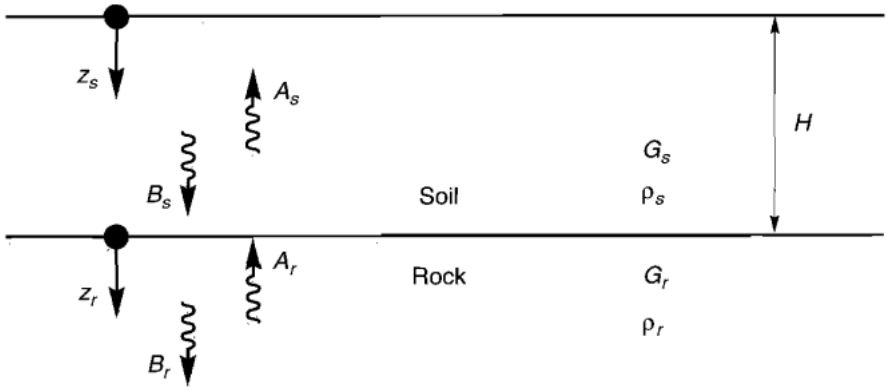

Figure 4.6 Soil Layer Overlaying on Top of a Half-Space Elastic Rock [37]

$$\frac{G_s k_s{}^*}{G_r k_r{}^*} A_s(e^{i(k_s{}^* H)} - e^{-i(k_s{}^* H)} = A_r - B_r \tag{4.22}$$

The ratio:

$$\frac{G_s k_s{}^*}{G_r k_r{}^*} = \rho \frac{\rho_s V_{s,s}}{\rho_r V_{s,r}} = \propto_z{}^* \tag{4.23}$$

Where $\propto_z{}^*$ is the complex impedance ratio, and $V_{s,s,}$ and $V_{s,r}$ are the soils and rock's complex shear wave velocities, respectively.

$$A_r = \frac{1}{2} A_s[(1 + \propto_z{}^*)e^{i(k_s{}^* H)} + (1 - \propto_z{}^*)e^{-i(k_s{}^* H)}] \tag{4.24}$$

$$B_r = \frac{1}{2} A_s[(1 - \propto_z{}^*)e^{i(k_s{}^* H)} + (1 + \propto_z{}^*)e^{-i(k_s{}^* H)}] \tag{4.25}$$

Assume that a shear wave with amplitude *A* and vertical propagation passed through the rock. Without soil, the free surface effect at the rock outcrop would result

in a motion of the bedrock outcropping, with an amplitude of *2A*, the free surface motion amplitude would be with the soil present.

$$2A_s = \frac{4A_r}{(1+\propto_z{}^*)e^{i(k_s{}^*H)}+(1-\propto_z{}^*)e^{-i(k_s{}^*H)}} \tag{4.26}$$

Defining the transfer function, *F*, as the ratio of the soil surface amplitude to the rock outcrop amplitude:

$$\frac{A_s}{A_r} = F(\omega) = \frac{2}{(1+\propto_z{}^*)e^{i(k_s{}^*H)}+(1-\propto_z{}^*)e^{-i(k_s{}^*H)}} \tag{4.27}$$

Using Euler's law can rewrite the equation as:

$$F(\omega) = \frac{1}{cos(k_s{}^*H)+i\propto_z{}^* sin(k_s{}^*H)} = \frac{1}{\cos\left(\frac{\omega H}{Vs,s^*}\right)+i\propto_z{}^*\sin\left(\frac{\omega H}{Vs,s^*}\right)} \tag{4.28}$$

For comparison with case 1, we might rewrite the transfer function as follows if damping was assumed to be zero:

$$F(\omega, \xi = 0) = \frac{1}{\sqrt{cos^2(k_sH)+\propto_z{}^2 sin^2 k_sH)}} \tag{4.29}$$

Resonance will not occur because the denominator is always greater than zero, even when the soil is undamped. Figure 16 shows how the impedance ratio, which measures bedrock stiffness, affects amplification behavior. Compare the amplification factor curves in Figure 16 to show how similar the effects of bedrock elasticity and soil damping are. The rock's flexibility influences the amplification.

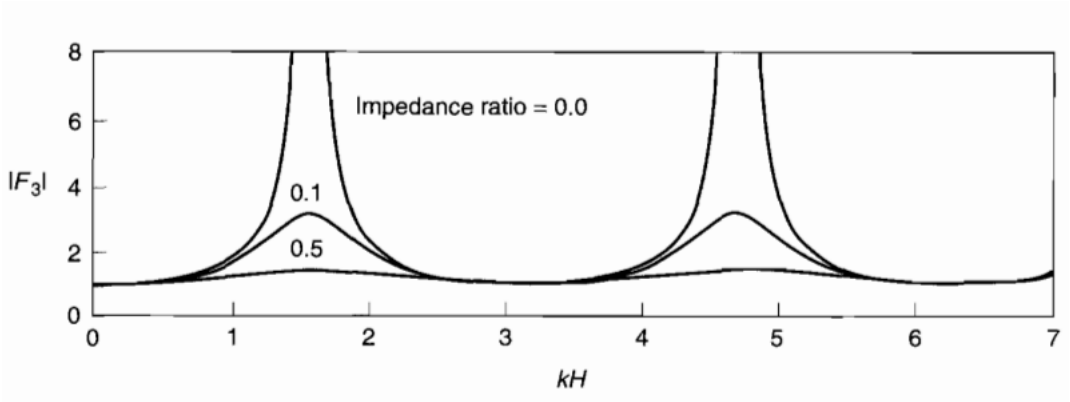

Figure 4.7 Impedance Ratios Impact on The Amplification Factor in The Undamped Soil [37]

4.7.4 Layered Damped Soil on Elastic Rock

While the uniform elastic layer models help illustrate how different ground motion characteristics are affected by soil conditions, they are also appropriate for investigating practical ground response issues. Real ground response problems usually involve soil layers with varying stiffness and damping properties and boundaries at which elastic wave energy will be reflected and transmitted. The transfer function development for multilayer soil deposits is necessary under these circumstances. Consider a soil deposit with N horizontal layers, the N_{th} layer being bedrock Figure 17.

Using a local coordinate system, *Z*, the displacement at the top and bottom of layer *m* will be the solution to the wave equation for each layer.

$$u_m = u_m(z_m, t) = A_m e^{i(\omega t + {k_m}^* z_m)} + B_m e^{i(\omega t - {k_m}^* z_m)} \qquad (4.30)$$

Where *A* and *B* stand for the amplitude of waves moving in opposite directions upward $+Z$ and downward -*Z*, respectively

$$u_{m+1} = u_{m+1}(z_{m+1}, t) = A_{m+1} e^{i(\omega t + {k_{m+1}}^* z_{m+1})} + B_{m+1} e^{i(\omega t - {k_{m+1}}^* z_{m+1})} \qquad (4.31)$$

At layer boundaries, displacement must be compatibility. It means that displacement at the top of the layer must be equal to the displacement at the bottom of

the layer. Applying the condition for compatibility to the transition between layer *m* and layer *m+1* or yield.

$$u_m(z_m = h_m) = u_{m+1}(z_{m+1} = 0)\ and\ \tau_m(z_m = h_m) = \tau_{m+1}(z_{m+1} = 0) \qquad (4.32)$$

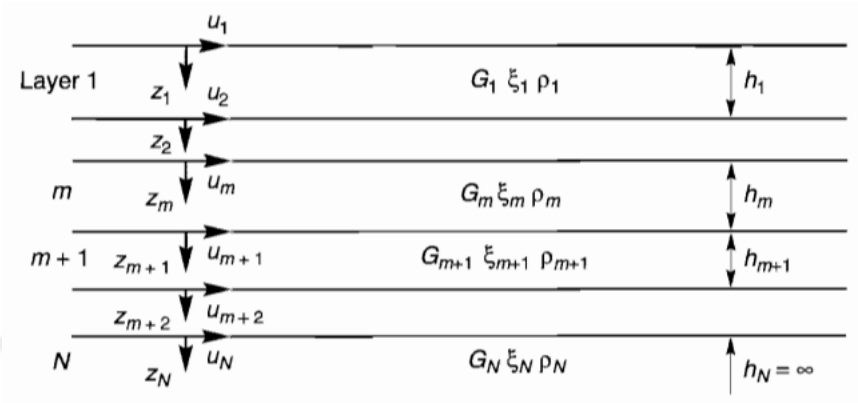

Figure 4.8 Layer of Soils Over Elastic Bedrock [37]

$$A_m(e^{i(k_m{}^* h_m)} + B_m e^{-i(k_m{}^* h_m)} = A_{m+1} + B_{m+1} \qquad (4.33)$$

The shear stresses at the top and bottom of layer *m* are:

$$\tau_m(z_m = h_m, t) = \tau_{m+1}(z_{m+1} = 0, t) \qquad (4.34)$$

$$A_{m+1} - B_{m+1} = \frac{k_m G_m{}^*}{k_{m+1}{}^* G_{m+1}{}^*} A_m(e^{i(k_m{}^* h_m)} - e^{-i(k_m{}^* h_m)} \qquad (4.35)$$

Adding (4.33) and (4.35) and subtracting (4.35) from (4.33) gives the recursion formulas:

$$A_{m+1} = \frac{1}{2} A_m[(1 + \propto_m{}^*) e^{i(k_m{}^* h_m)} + \frac{1}{2} B_m(1 - \propto_m{}^*) e^{-i(k_s{}^* h_m)}] \qquad (4.36)$$

$$B_{m+1} = \frac{1}{2} A_m[(1 - \propto_m{}^*) e^{i(k_m{}^* h_m)} + \frac{1}{2} B_m(1 + \propto_m{}^*) e^{-i(k_s{}^* h_m)} \qquad (4.37)$$

Where $\propto_m{}^*$ is the complex impedance ratio at the boundary between layers *m* and *m + 1*:

$$\propto_m{}^* = \frac{k_m G_m{}^*}{k_{m+1}{}^* G_{m+1}{}^*} = \frac{\rho_s V_{s,m}{}^*}{\rho_{m+1}(V_{s,)m+1}{}^*} \qquad (4.38)$$

Since the shear stress at the ground surface must be zero and A_1 equal to B_1. Functions linking the amplitude in layer 1 can be expressed by applying the recursion formulas of equation (4.36) again for all layers from 1 to *m*.

$$A_m = a_m(\omega)A_1 \tag{4.39}$$

$$B_m = b_m(\omega)B_1 \tag{4.40}$$

The transfer function relating the displacement amplitude at layer *i* to that at layer *j* is given by:

$$F_{ij}(\omega) = \frac{u_i}{u_j} = \frac{a_i(\omega)+b_i(\omega)}{a_j(\omega)+b_j(\omega)} \tag{4.41}$$

The amplification of acceleration and velocities from layer *i* to layer *j* is described by equation (4.41). According to equation (4.41), it is possible to understand the motion of any other layer. Therefore, the motion at any other location in the soil profile can be contributed if the motion at any other point is known. As a result, it is possible to do the deconvolution operation, which is highly beneficial.

4.8 Description and Analysis Procedure In DEEPSOIL

In this section, numerical modeling is used to try to simulate the soil amplification of the structure. The DEEPSOIL one-dimensional SRA program, which is widely used in equivalent linear and non-linear one-dimensional seismic SRA, was used to model the soil profile of the selected example. Significant conclusions about the impact of local site situation on seismic wave propagation have been drawn by an equivalent linear approach.

In the analysis, Groholski [41] proposed the general quadratic/hyperbolic model (GQH) which is employed to define the backbone curve shape for the stress-strain relationship. Non-masing hysteresis models are used to reduce loop size and replicate the behavior of the soil under laboratory conditions. Two sets of equations can be used to explain the hyperbolic model. The stress-strain expression for loading is defined by the first relation, known as the backbone curve, and for unloading and reloading conditions, the second equation defines the stress-strain relationship. Both equations show the loading and unloading modified Konder Zelasko (MKZ) model [42]:

$$\tau = \frac{\gamma * G0}{1+\beta(\frac{\gamma}{\gamma r})\hat{}s} \quad (4.42)$$

$$\tau = \frac{2*G0(\frac{\gamma - \gamma r}{2})}{1+\beta(\frac{\gamma - \gamma r}{2*\gamma r})\hat{}s} + \tau rev \quad (4.43)$$

Where γ is shear strain γr is the reference shear strain, G_0 is the ultimate shear coefficient, and S is a dimensionless exponent.

When soil is unloaded or reloaded, several models use the masing rules [43] to explain the hysteretic response. The following are the four expanded masing rules:

- The stress-strain curve follows the backbone curve for initial loading:

  $\tau = F_{bb}(\gamma)$ (4.44)

  where τ shows the shear stress, $F_{bb}(\gamma)$ indicates the backbone curve.
- The stress-strain curve has the following path when the stress reversal happens at a point:

  $$\frac{\tau - \tau \text{ rev}}{2} = Fbb\left(\frac{\gamma - \gamma rev}{2}\right) \quad (4.45)$$
- If the backbone curve crosses the off-loading or reloading graph, the off-loading or reloading graph will be followed until the next stress reversal.
- When an unloading or reloading curve intersects with earlier cycles, the stress-strain curve follows the previous cycles.

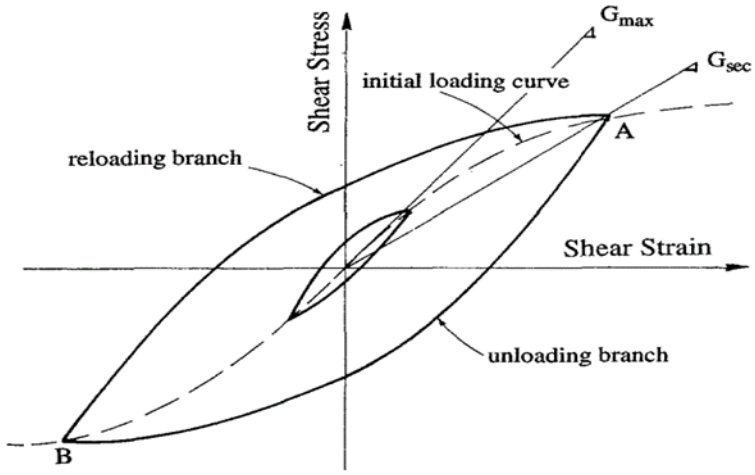

Figure 4.9 Relationship of Soil Stress and Strain During Cyclic Shear Deformation [16]

Response analysis was performed to model soil behavior using Derendelis [44] empirical modulus reduction and damping curves. Modulus reduction and damping curves were fitted using the MRDF method.

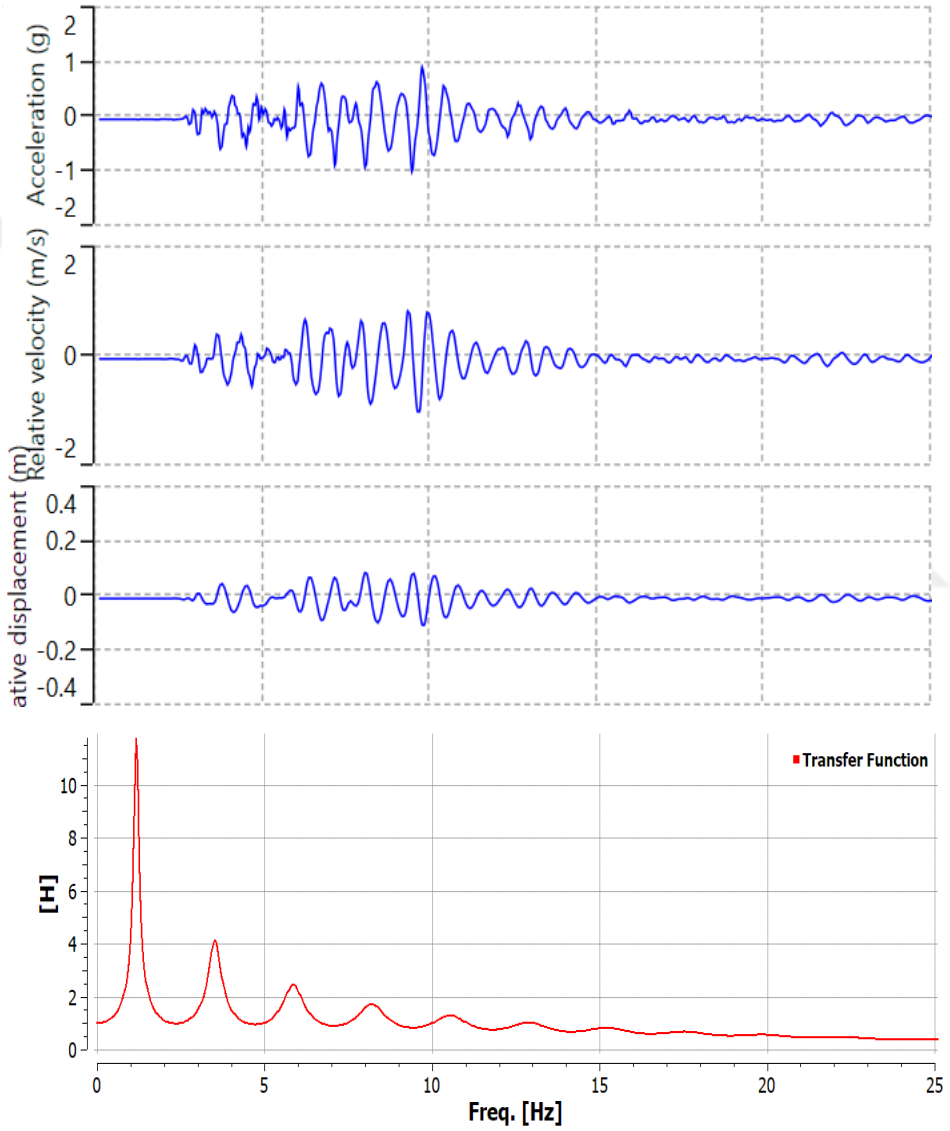

Figure 4.10 Linear Result Analyse of SA of Imperial Valley-06

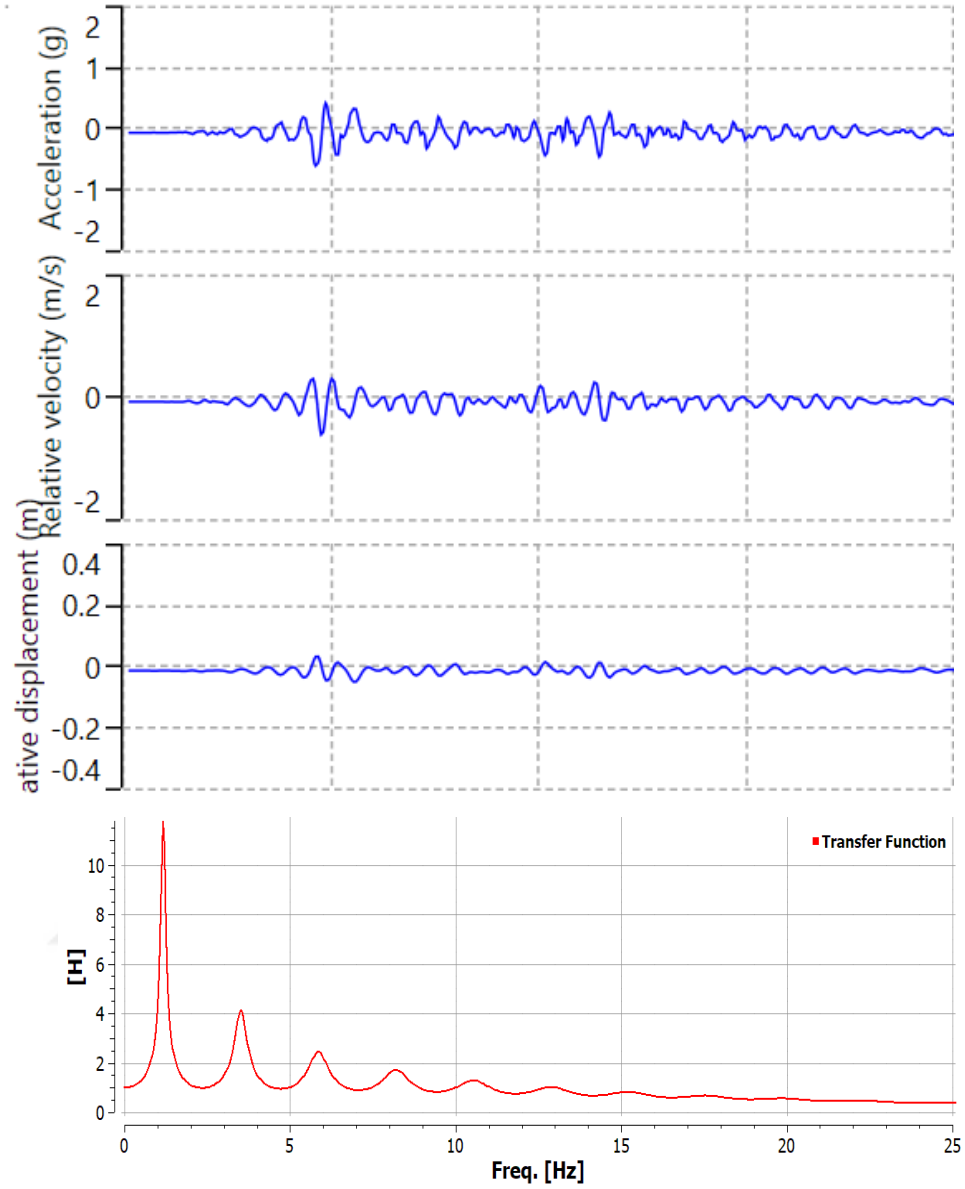

Figure 4.11 Result of Linear Analysis of SA of Italy-01

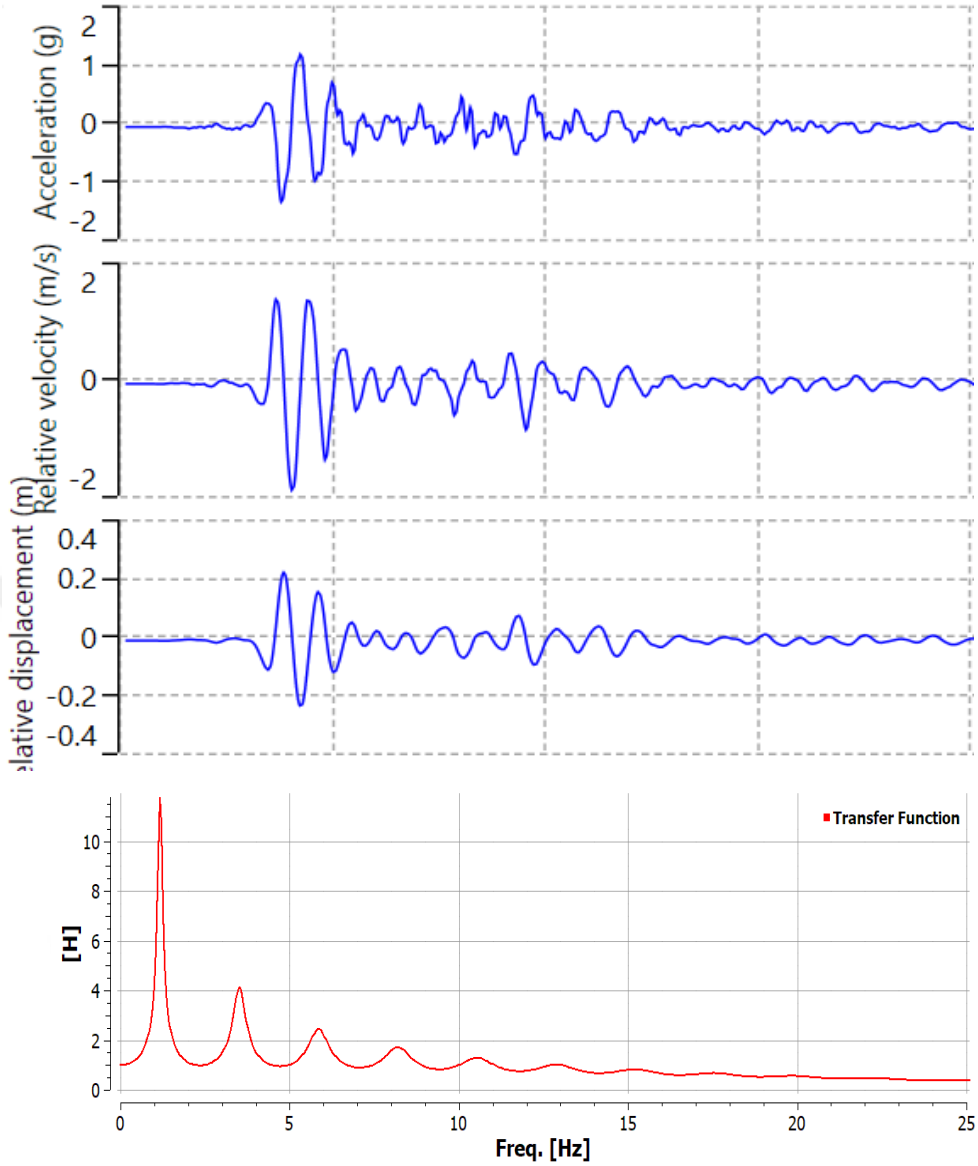

Figure 4.12 Result of Linear Analysis of SA of Northridge

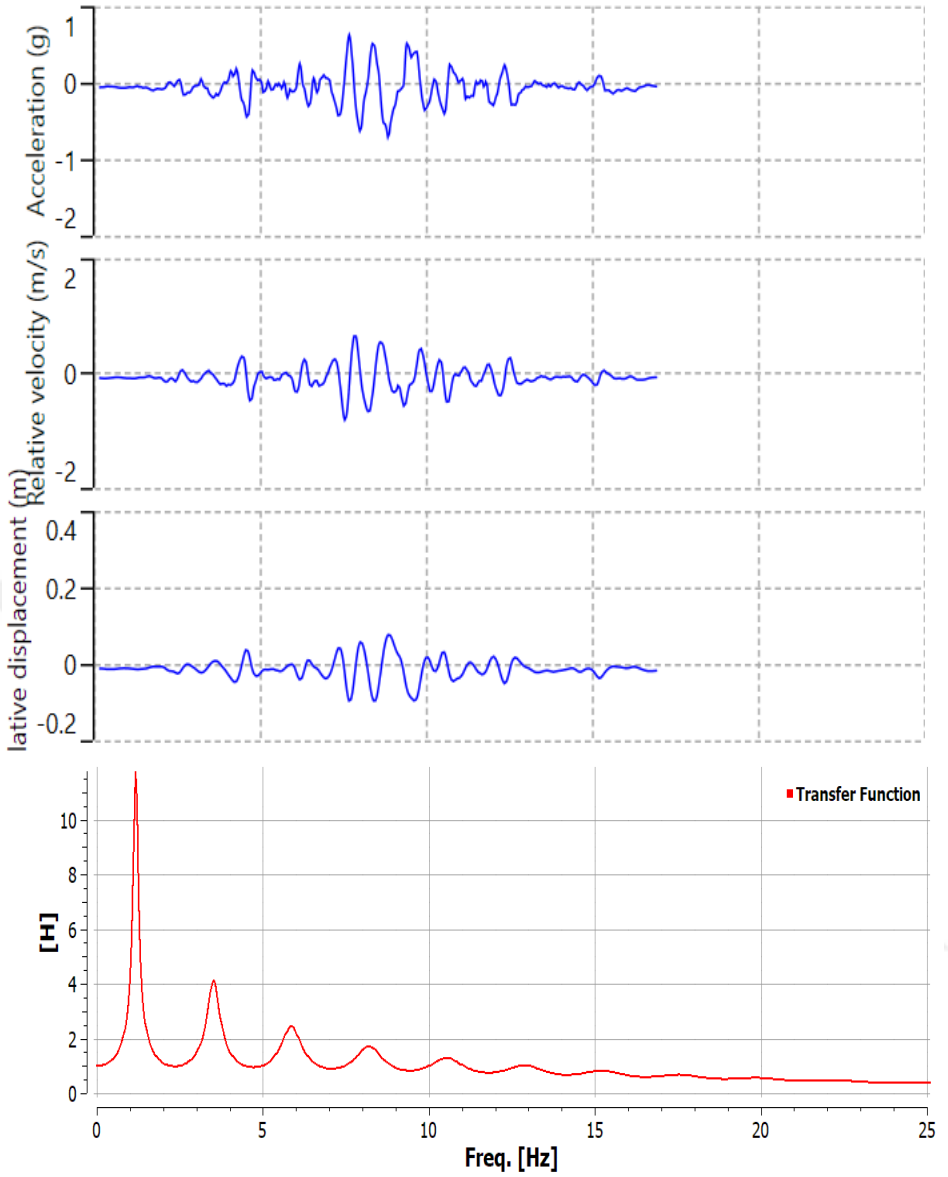

Figure 4.13 Linear Result Analyse of SA of Superstition Hills-02

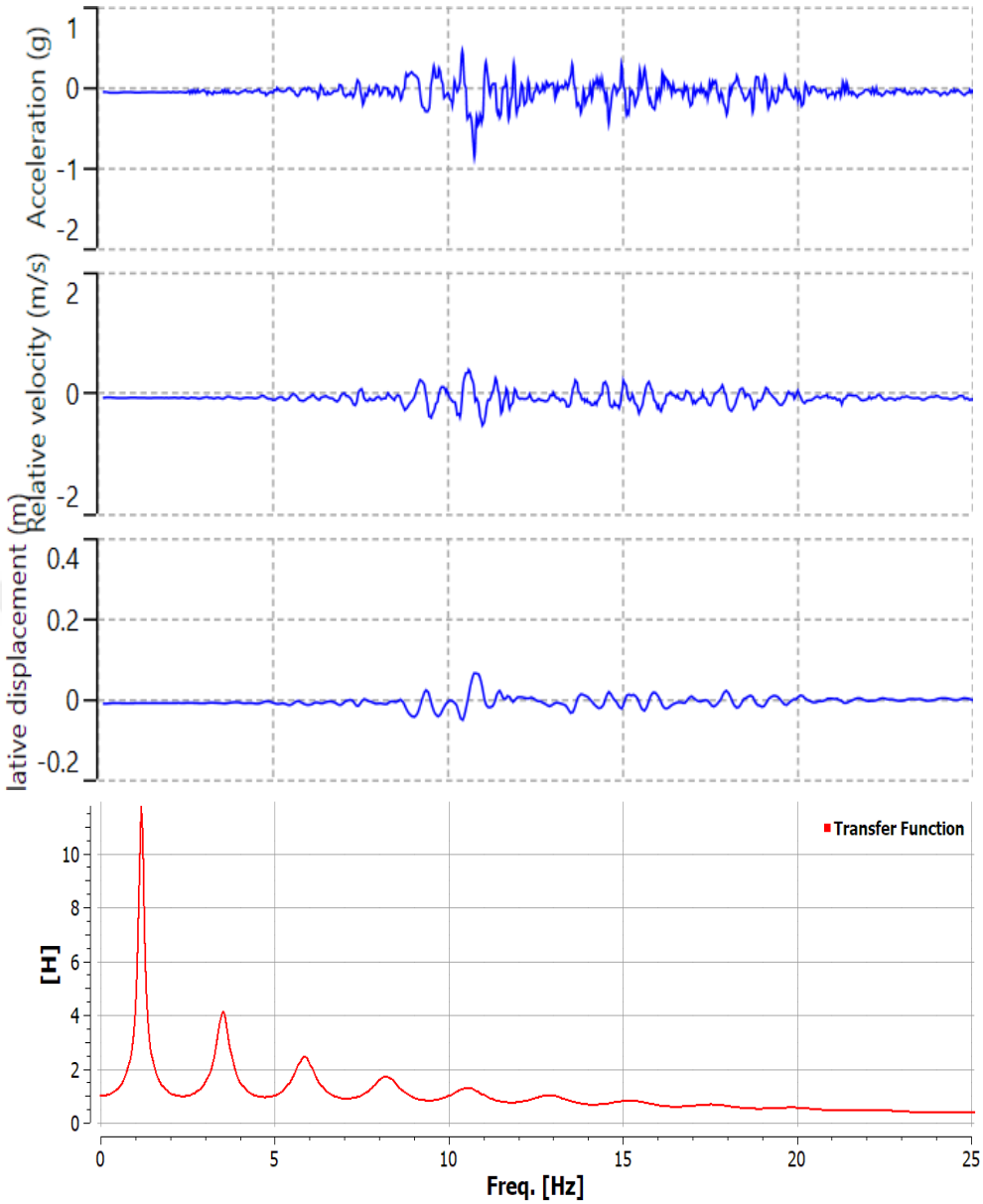

Figure 4.14 Linear Result Analyse of SA of Londers

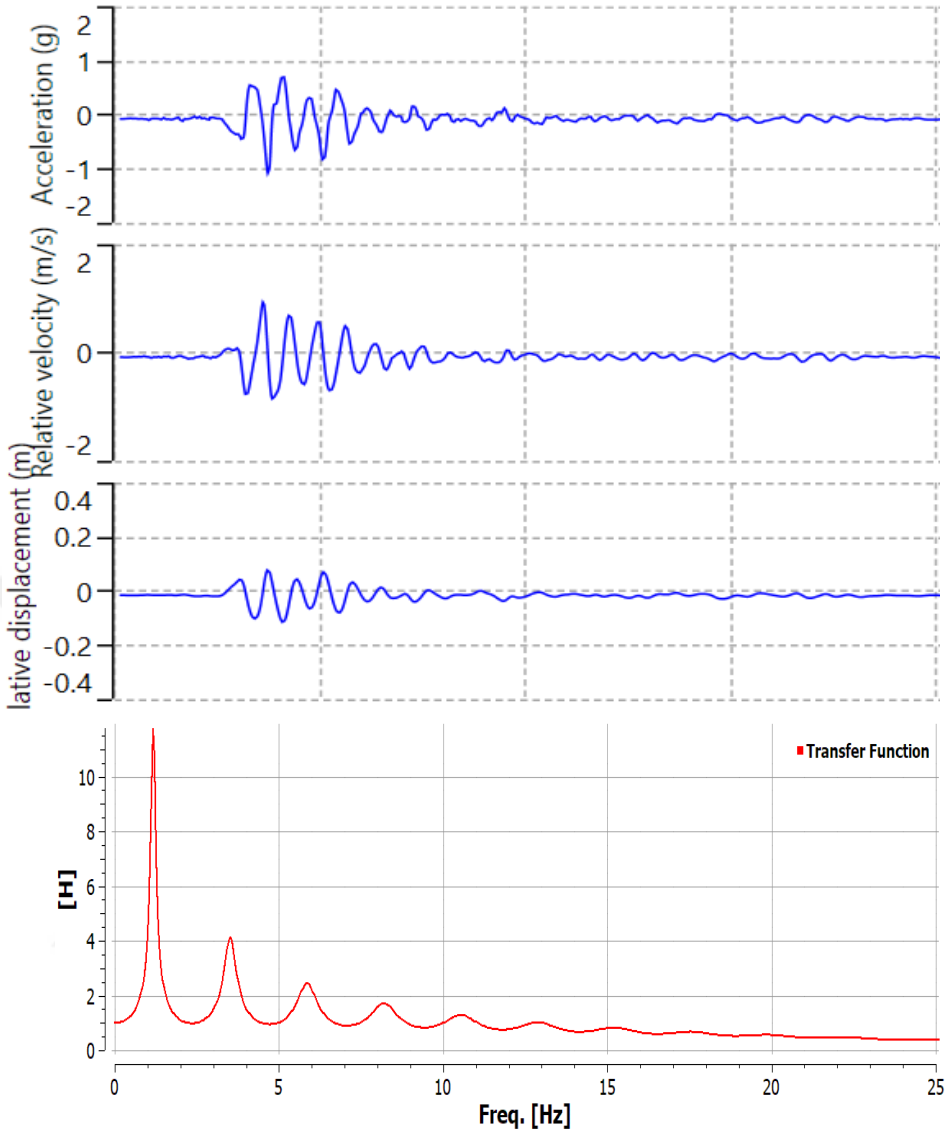

Figure 4.15 Linear Result Analyse of SA of Erzincan

The second type of soil, as mentioned in section 4.7.2 of this chapter, homogeneous damped soil on a rigid rock, is used to check soil response against six earthquake motions. This research used a single layer with 30 m height and 350 m/sec shear wave velocity for analyzing the soil with a density and damping ratio of 20 KN/m^3 and 0.05, respectively. In this study, DEEPSOIL was used for analyzing the soil. The finding shows that the earthquake motion data with high PGA has more impact on the structure and has high acceleration, velocity, and displacement, as shown in Figures 19-24. The transfer function shows that due to the damping ratio, resonance will not occur, and the frequency of the ground motion will de-amplify.

CHAPTER V

Numerical study

The impact of soil on the seismically isolated structure model is discussed in this section. As mentioned in the previous chapter, the SA model is carried out by DEEPSOIL, and base isolation is modeled by MATLAB software. Non-linear time history analysis was utilized in this study to analyze the base-isolated structure. The Bouc-Wen hysteretic model was used to model the idealized hysteresis loop for LRB. It was proposed first time by Bouc [33], but it was Wen [34] who expanded on it by creating a variety of hysteretic patterns. The study is aimed to comprehend the effect of SA on the structural response of the isolated structure and to reduce the dynamic properties of the structure by providing base isolation. After the modeling and analysis, the results are presented as the bearing force of the LRB, ground acceleration, bearing displacement, and story drift.

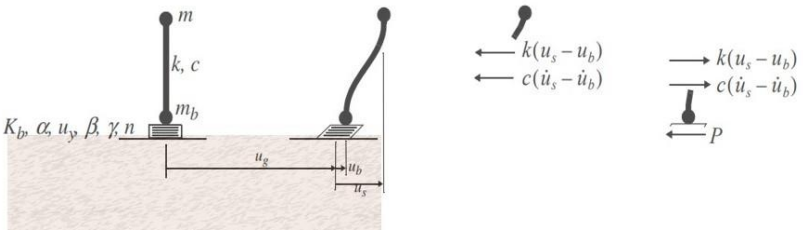

Figure 5.1 SDOF Structure on Lead Rubber Bearing [45]

5.1 Time History Analysis

Time-history analysis provides for linear or nonlinear evaluation of dynamic structural response under loading which may vary according to the specified time function vs acceleration format. This study applied six near-field seismic events uni-directionally to the seismically isolated structure. Each earthquake event was obtained from the Pacific Earthquake Engineering Research (PEER) Center.

Table 5.1 Ground Excitation Records

NO	Event	Station Name	RSN	Year	Mw	PGA (g)	PGV(m/s)	PGD (m)	predominant period (sec)
1	Imperial valley-06	Bonds Corner	160	1979	6.5	0.6	0.47	0.2	0.18
2	Italy-01	Sturno (STN)	292	1980	6.2	0.23	0.37	0.13	0.3
3	Superstition Hills-02	Parachute Test Site	723	1952	7.36	0.43	1.00	0.38	0.28
4	Erzincan, Turkey	Erzincan	821	1992	6.9	0.5	0.78	0.28	0.12
5	Landers	Lucerne	879	1992	7.3	0.73	1.3	1.1	0.04
6	Northridge-01	LA - Sepulveda VA Hospital	1004	1994	6.7	0.75	0.78	0.12	0.26

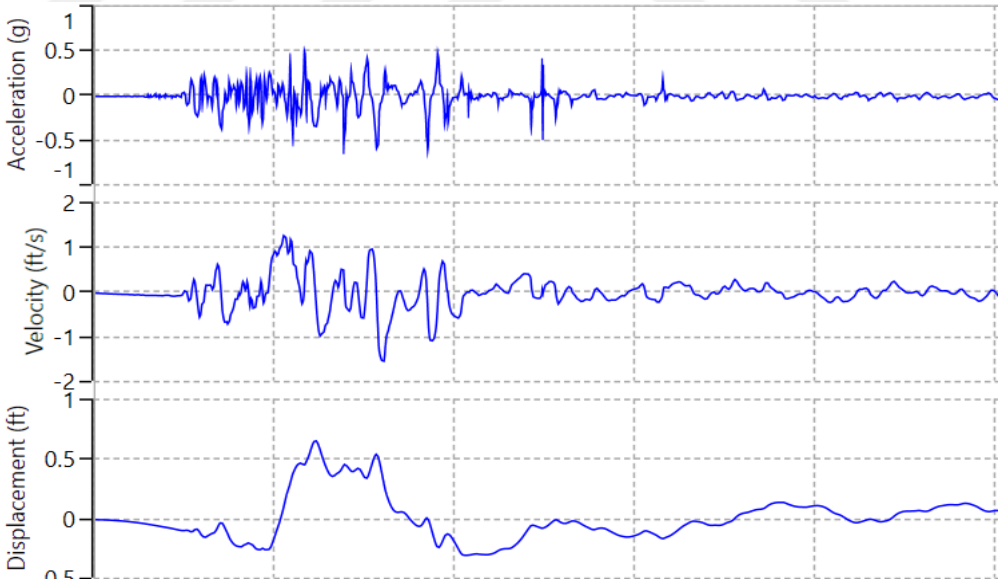

Figure 5.2 Imperial valley-06 Ground Motion

Figure 5.3 Italy-01 Ground Motion

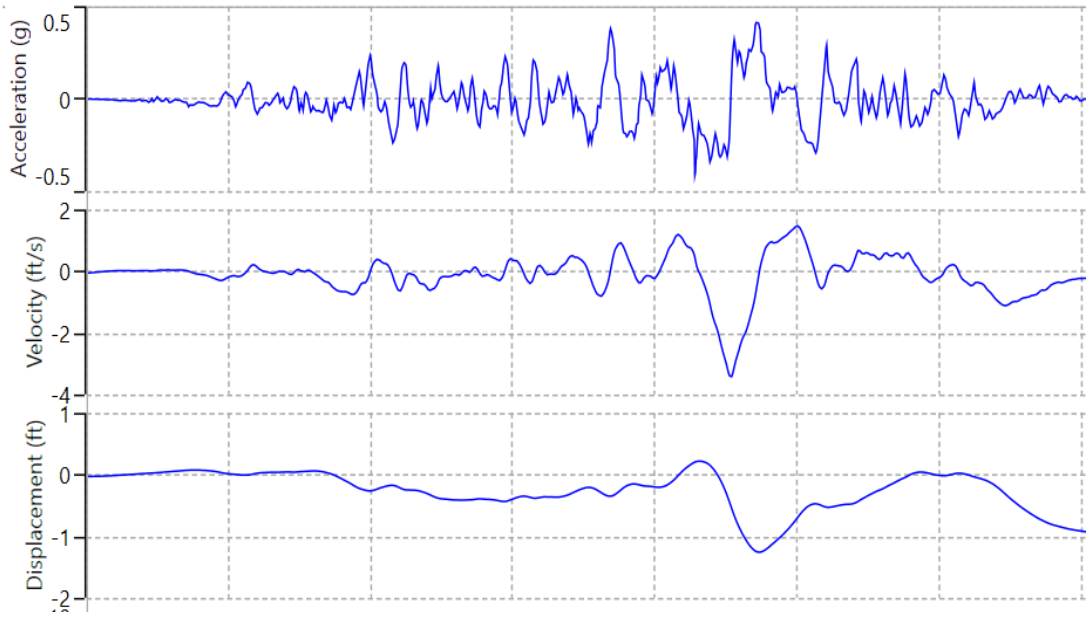

Figure 5.4 Superstition Hills-02 Ground Motion

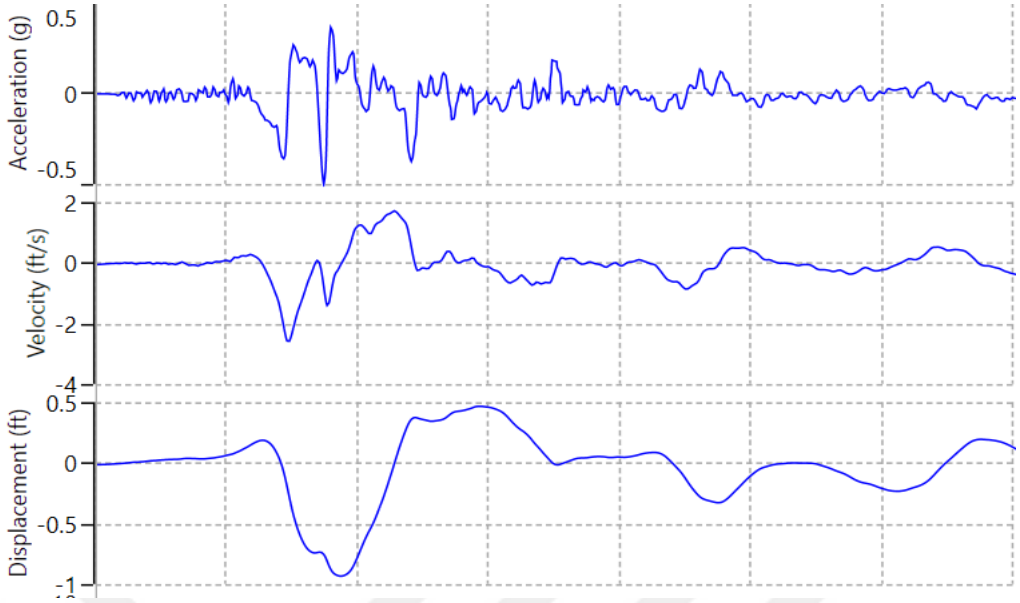

Figure 5.5 Erzincan Ground Motion

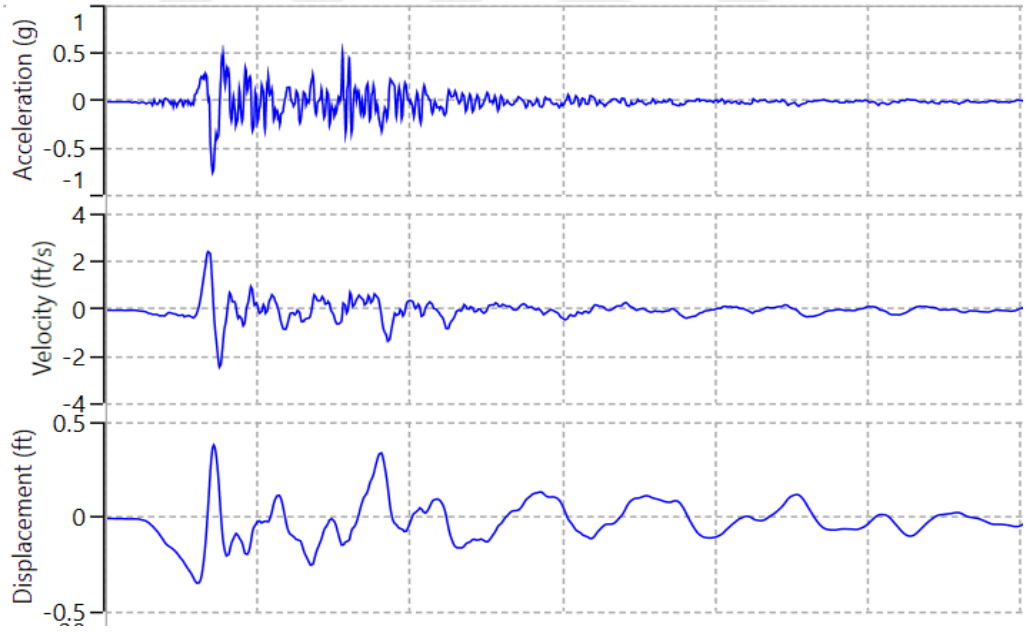

Figure 5.6 Northridge-01 Ground Motion

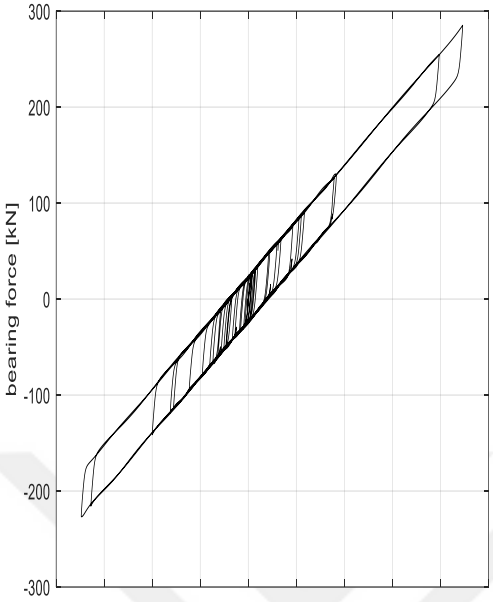

Figure 5.7 Bearing Force Without SA

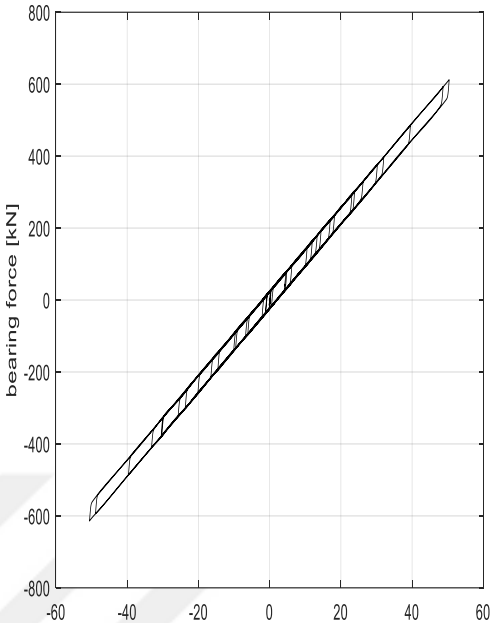

Figure 5.8 Bearing Force with Effect of SA

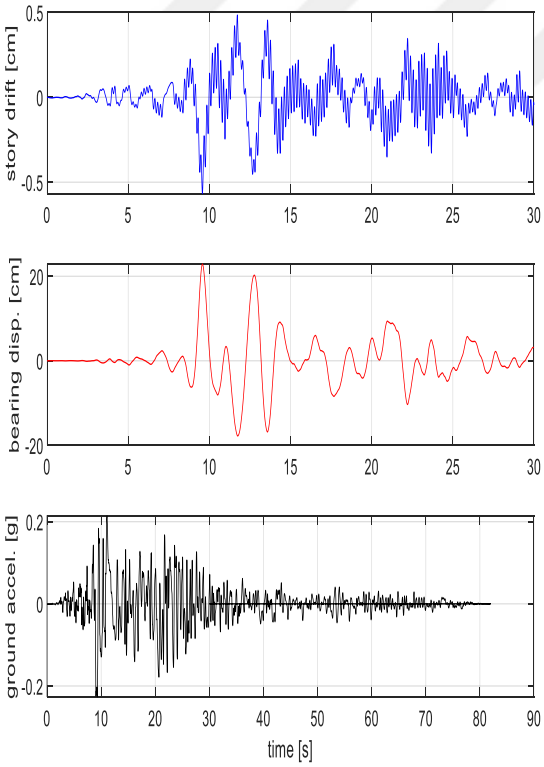

Figure 5.9 Result Analyses of Italy-01 Without SA

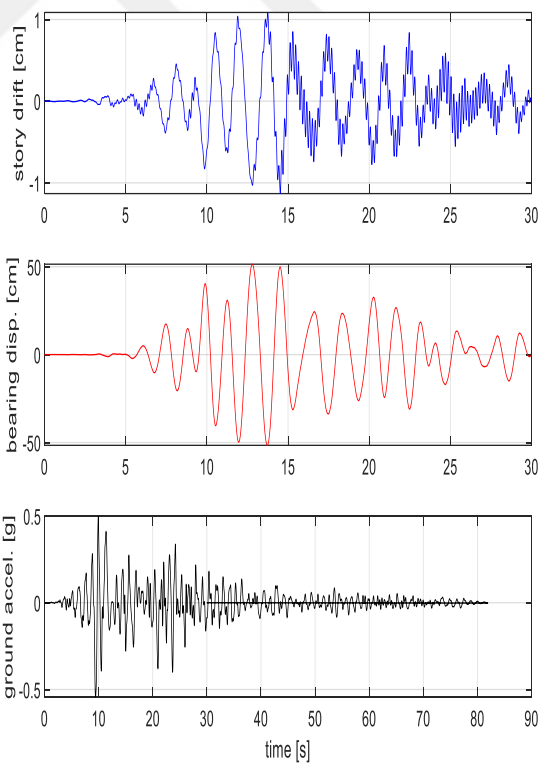

Figure 5.10 Result Analyses of Italy-01 with SA

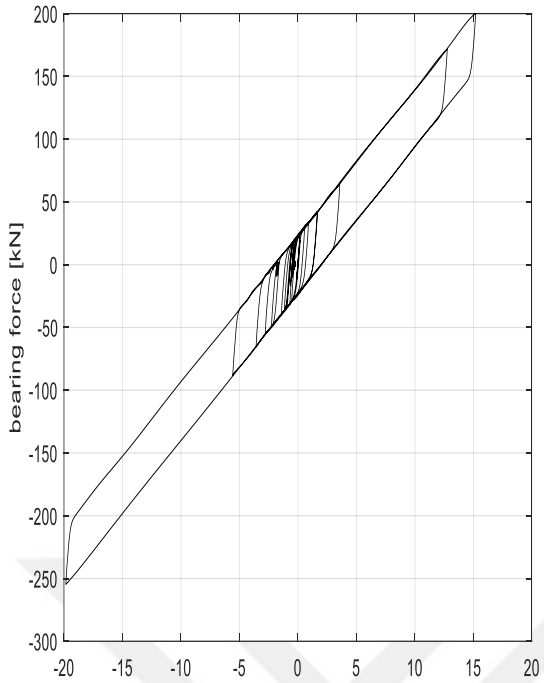

Figure 5.11 Bearing Force Without SA

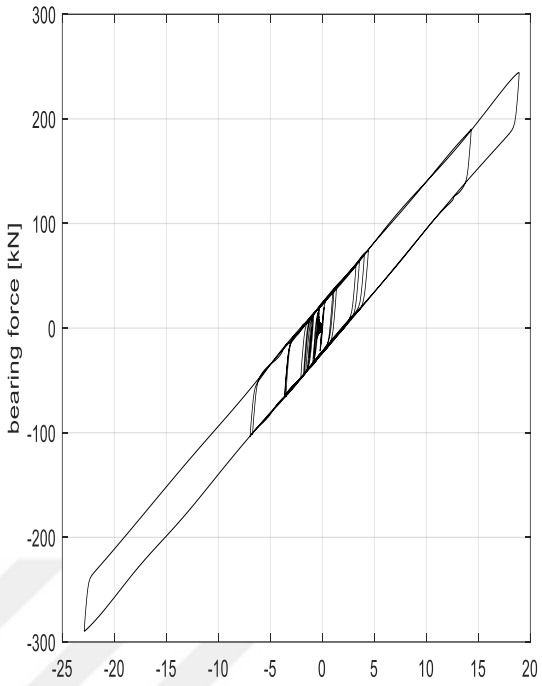

Figure 5.12 Bearing Force With SA

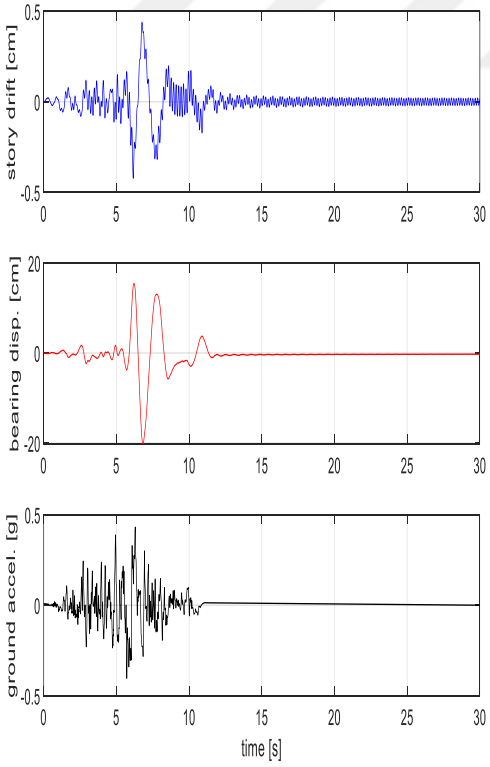

Figure 5.13 Result Analyses of Superstition Hills-02-723 Without SA

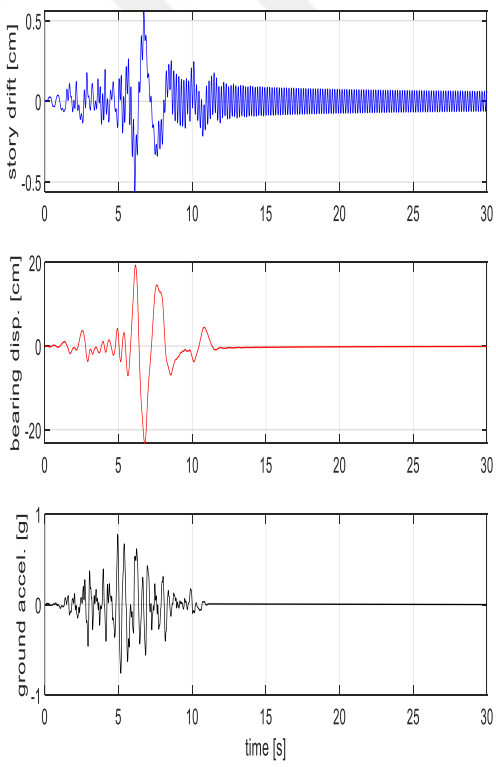

Figure 5.14 Result Analyses of Superstition Hills-02-723 With SA

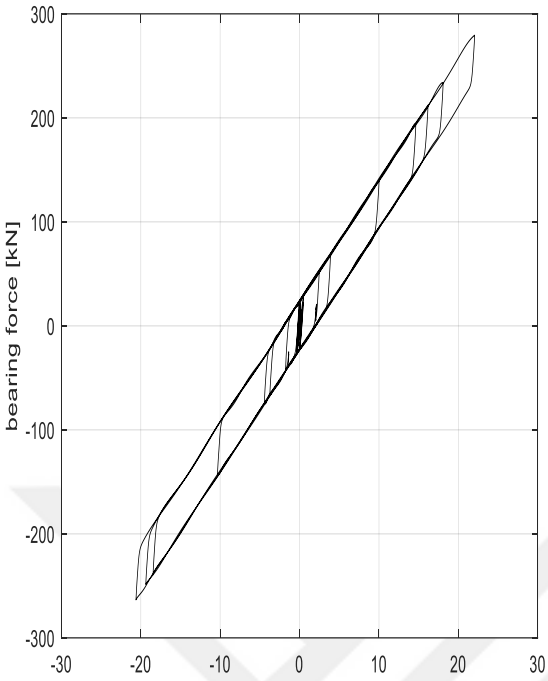

Figure 5.16 Bearing Force Without SA

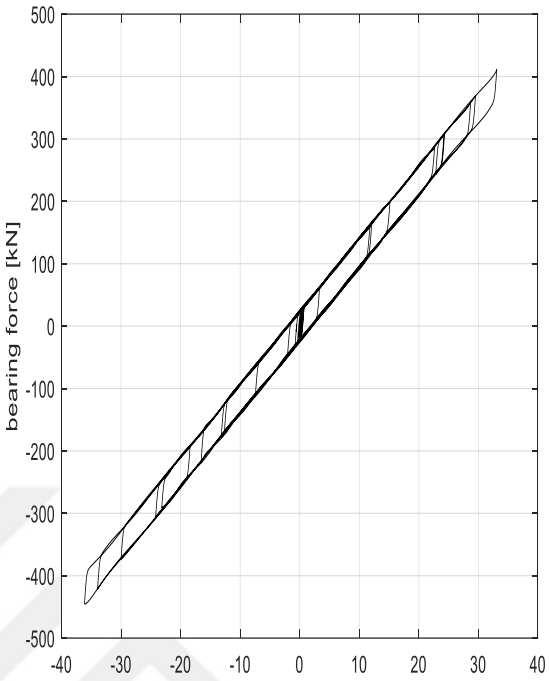

Figure 5.15 Bearing Force with SA

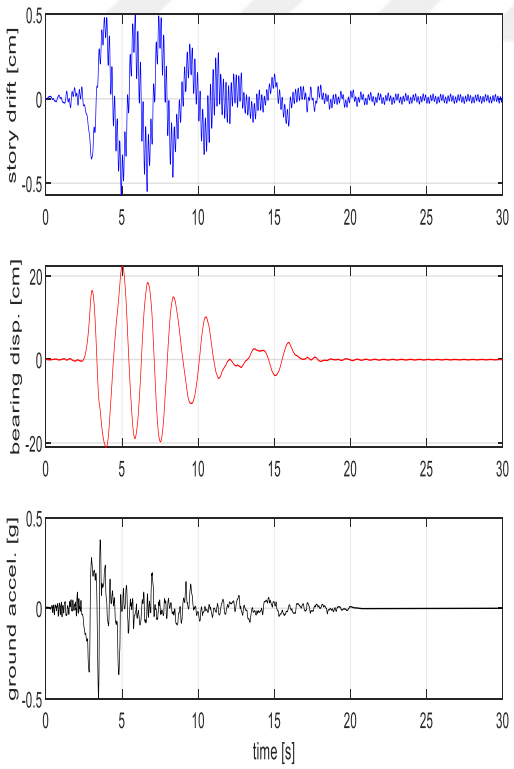

Figure 5.17 Result Analyses of Erzincan-821 Without SA

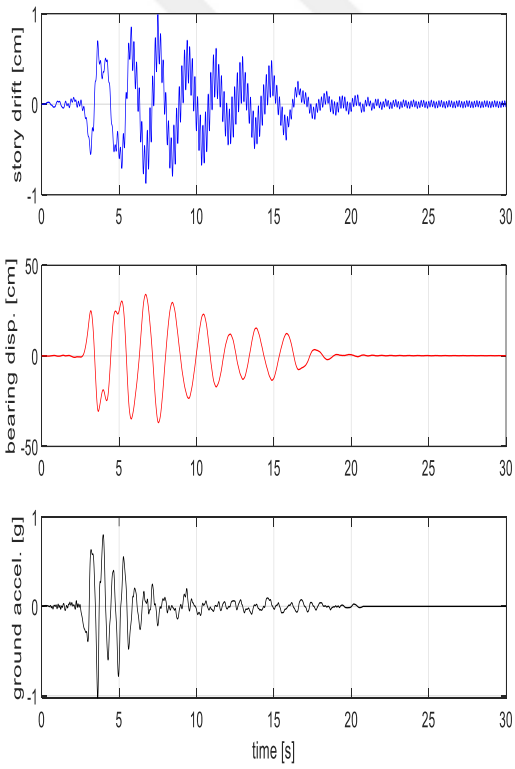

Figure 5.18 Result Analyses of Erzincan-821 with SA

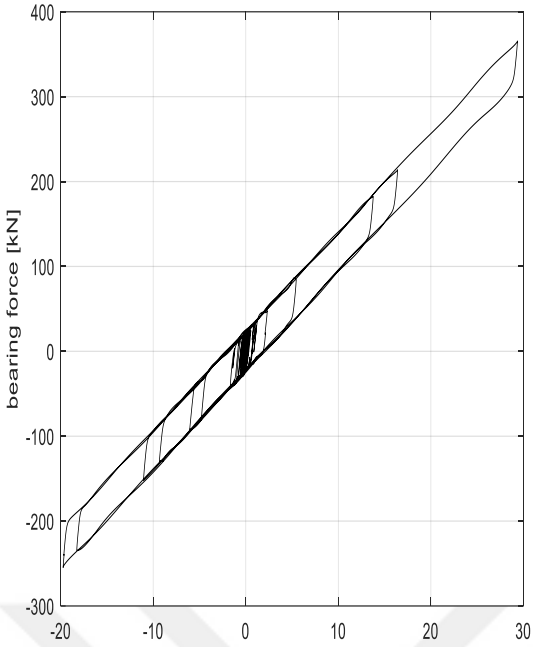

Figure 5.19 Bearing Force Without SA

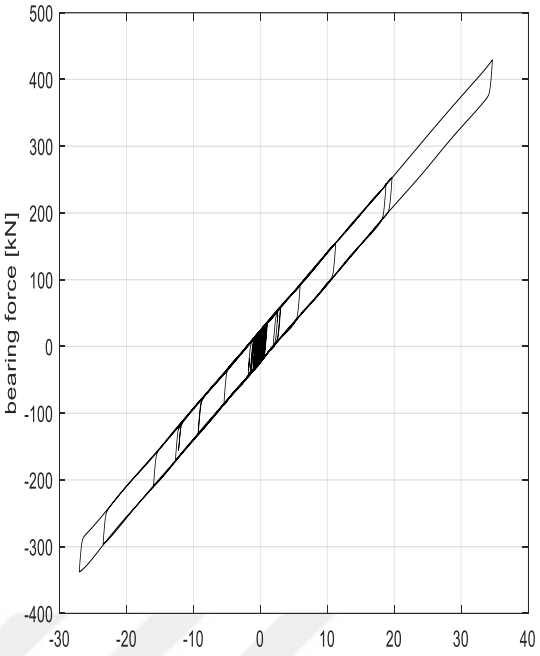

Figure 5.20 Bearing Force With SA

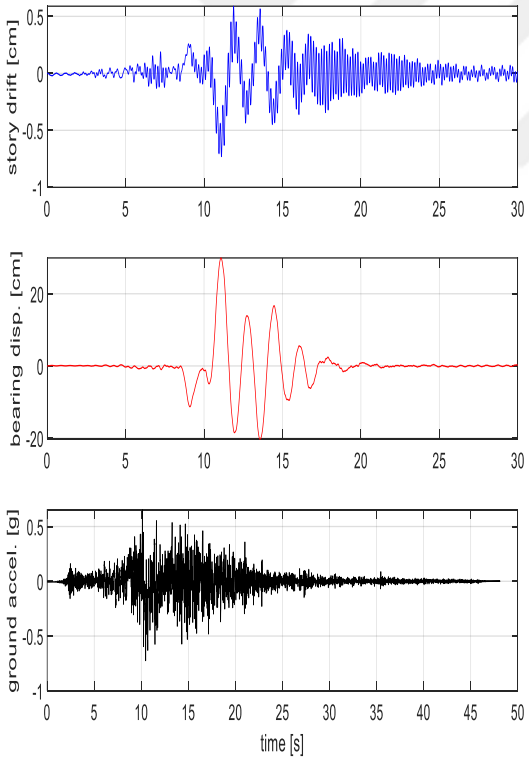

Figure 5.21 Result Analyses of Landers-879 Without SA

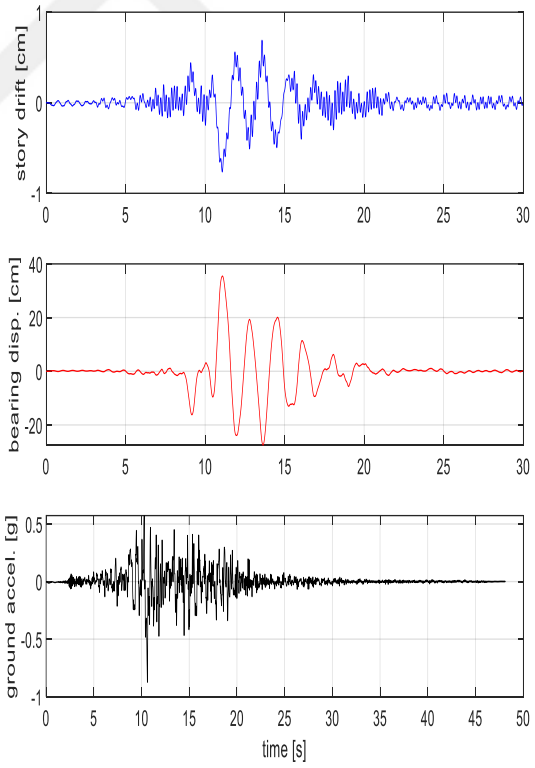

Figure 5.22 Result Analyses of Landers-879 With SA

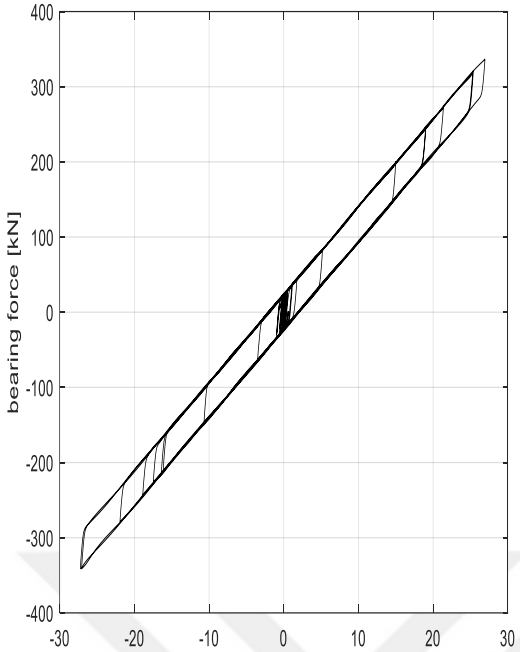

Figure 5.23 Bearing Force Without SA

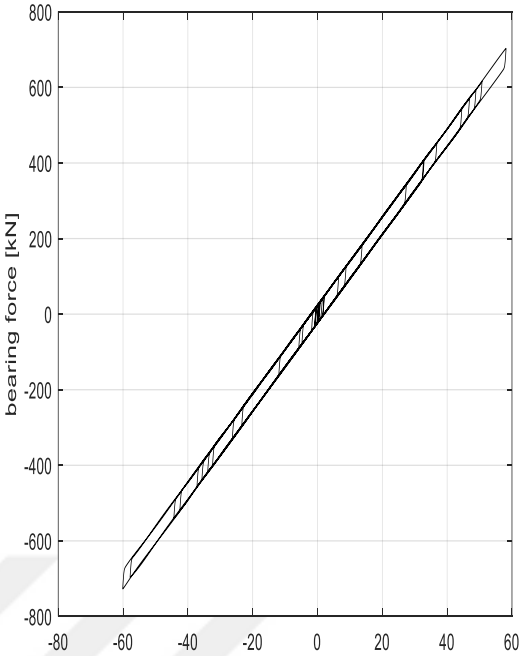

Figure 5.24 Bearing Force with SA

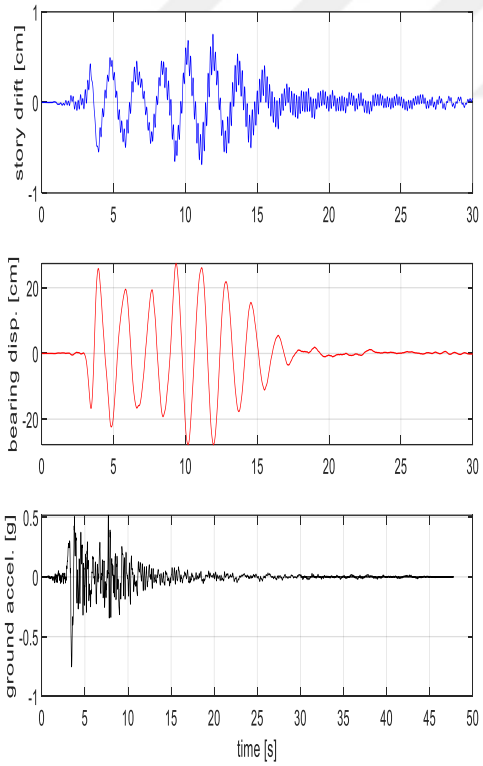

Figure 5.25 Result Analyses of Northridge-1004 Without SA

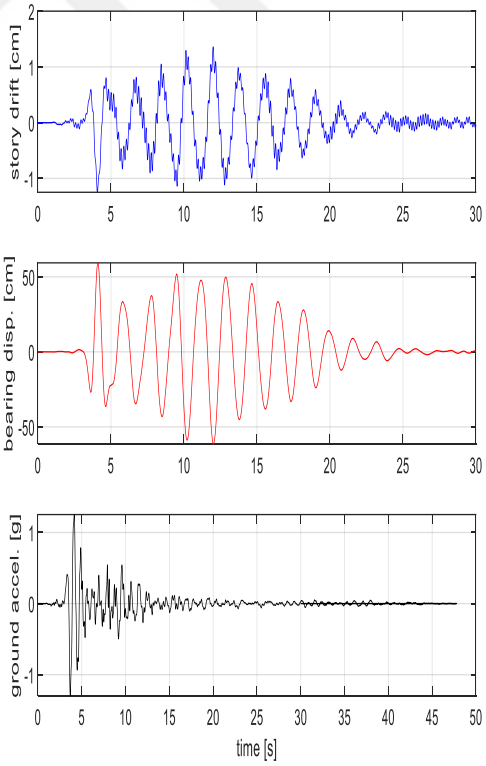

Figure 5.26 Result Analyses of Northridge-1004 with SA

CHAPTER VI

Result and Discussion

6.1 Overview

In this study, six near-fault earthquake ground motions were utilized to check the seismic response of the structure by considering soil amplification effects with LRB type of isolation. First, to demonstrate the influence of the soil on the structure, all six ground motions are applied to the base-isolated structure in MATLAB and check the results. Secondly, analyzing the soil considering the same ground motions on DEEPSOIL, and finally, taking the data of acceleration from the result of the analysis of DEEPSOIL and transferring it into MATLAB to check the response of the structure against earthquake by considering the impact of soil on the base-isolated structure.

In this research, the effect of soil on an isolated base structure is analyzed. As shown in ground motion data, the lowest value of PGA is 0.23g, and the highest PGA value is 0.75g. The bearing force results from all six ground motions show that soil amplifies the earthquake forces and increases the bearing displacements as shown in figures 31-50. Additionally, soil amplification had an influence on the shape and the area under the hysteresis loops of the bearings which is proportional to the energy dissipation capabilities of the seismic isolation system during an earthquake.

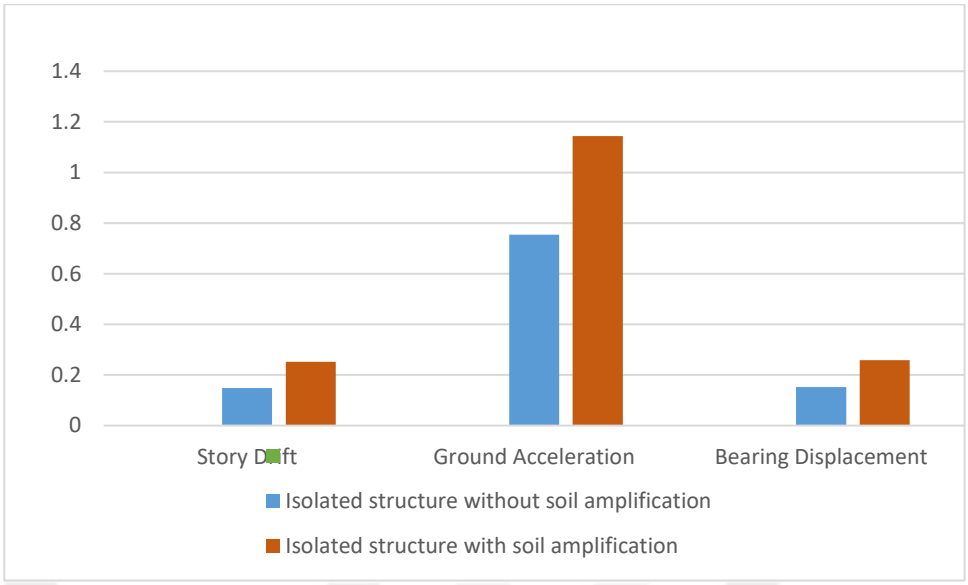

Figure 6.1 Imperial Valley-06 Ground Motion

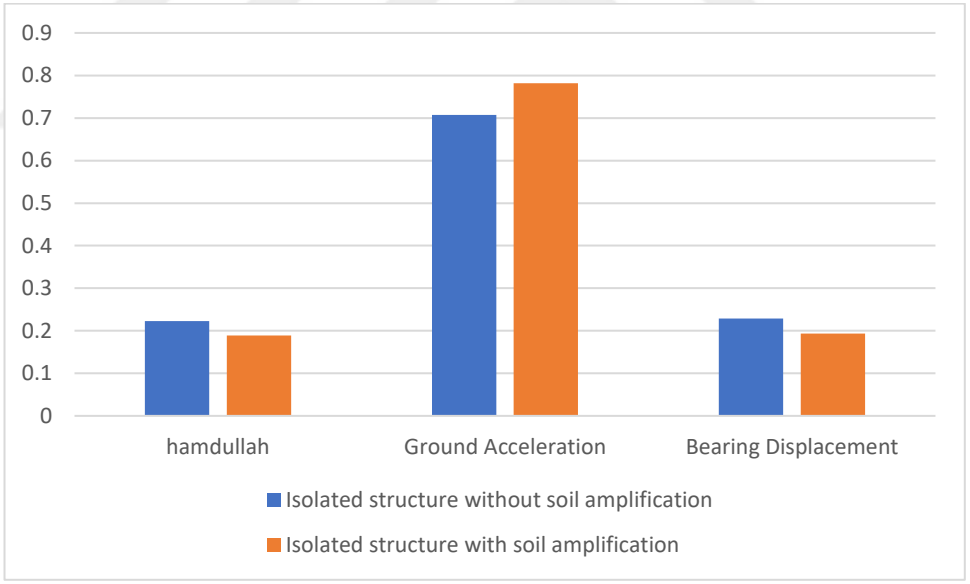

Figure 6.2 Italy-01Ground Motion

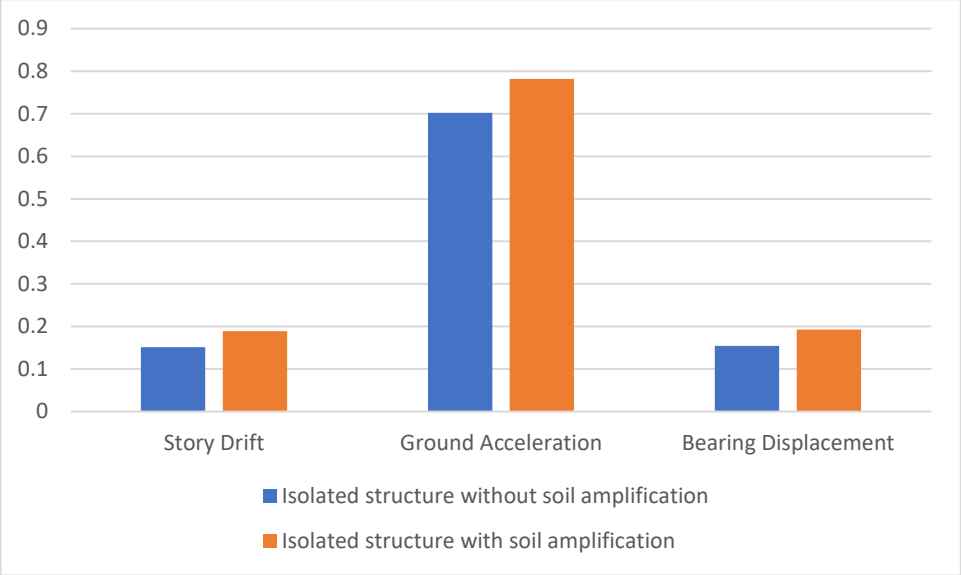

Figure 6.3 Superstition Hills-02-723 Ground Motion

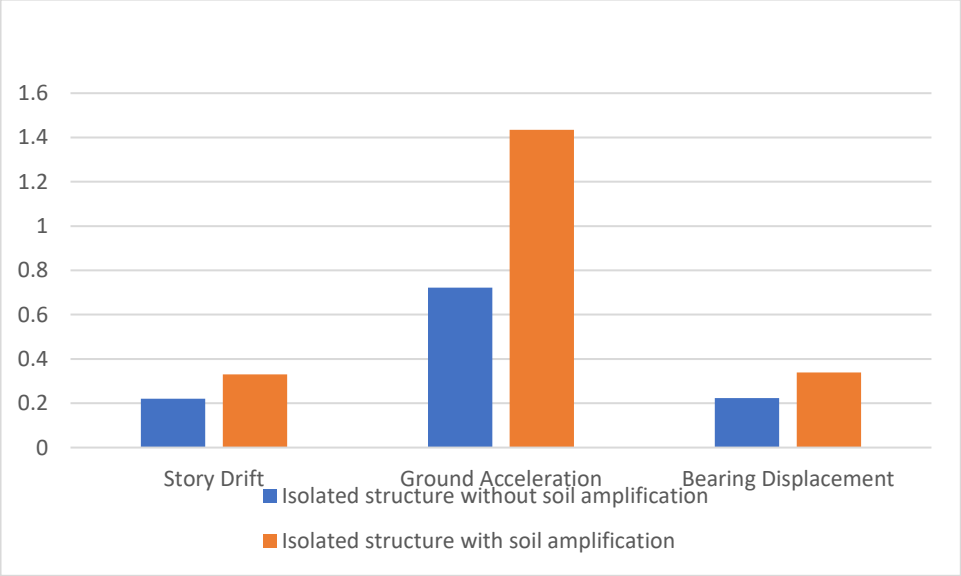

Figure 6.4 Erzincan-821 Ground Motion

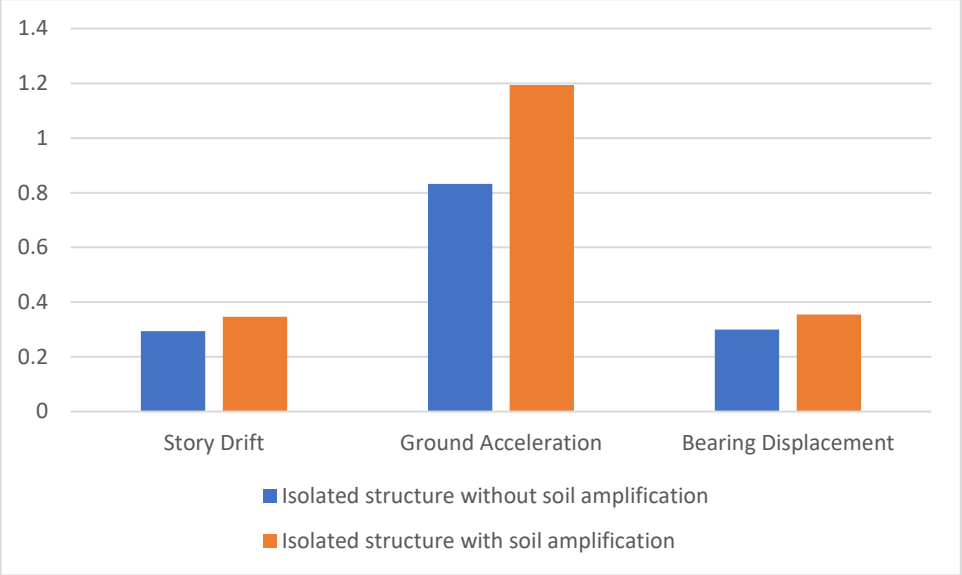

Figure 6.5 Landers-879 Ground Motion

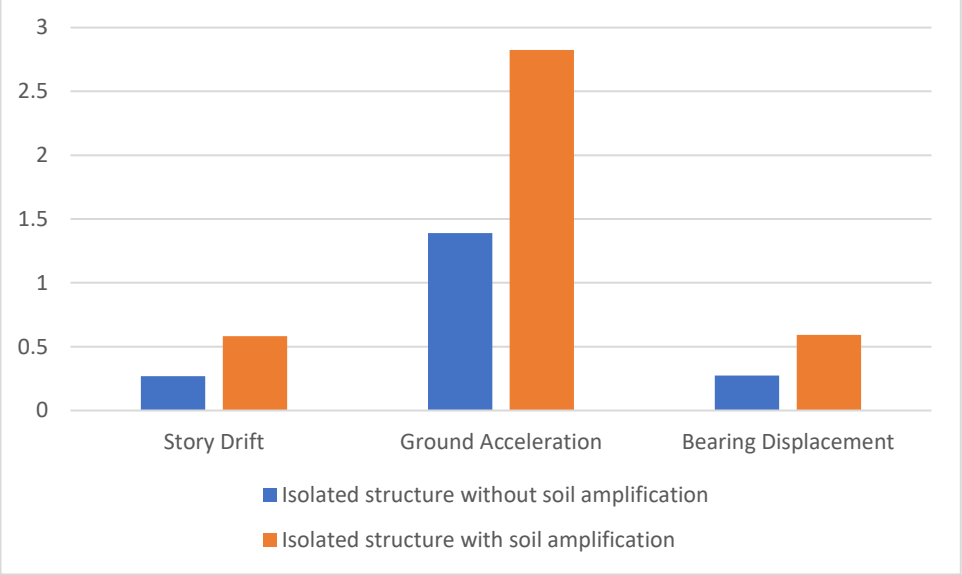

Figure 6.6 Northridge-1004 Ground Motion

CONCLUSION

This research focused on the effect of soil amplification on the response of a base-isolated structure model using six near-field seismic ground excitations. The seismic response of the structure was determined using non-linear response history analysis. The investigation's findings are as follows:

- In all cases, soil amplification increased the story drift, floor acceleration, and bearing displacement of the buildings.
- Soil amplification effects on the seismic response were more pronounced for the earthquake ground motions with high PGA.
- By analyzing the findings of the study, it can be seen that a base isolated structure without taking soil effect into account has less of an impact on ground excitation, but soil can magnify the effects of earthquakes on the structure.

This study investigated the influence of one-way soil structure interaction. As a result, using site response analysis to calculate the free surface ground motions can improve the prediction of the seismic response of isolated structures. The free surface ground accelerations were obtained using one dimensional linear site response analysis. The recommendation for future research is to use nonlinear site response analysis with two-way soil structure interaction to predict the seismic response of base isolated structures.

Reference

[1] Ellingwood, B. R. (2000). LRFD: implementing structural reliability in professional practice. *Engineering Structures*, *22*(2), 106-115.

[2] Nassar, A. A., Osteraas, J. D., & Krawinkler, H. (1992, July). Seismic design based on strength and ductility demands. In *10th World Conference on Earthquake Engineering* (Vol. 10, pp. 5861-5866).

[3] Lignola, G. P., Di Sarno, L., Di Ludovico, M., & Prota, A. (2016). The protection of artistic assets through the base isolation of historical buildings: a novel uplifting technology. *Materials and Structures*, *49*(10), 4247-4263.

[4] Jangid, R. S., & Datta, T. K. (1995). Seismic behavior of base isolated building: A state of art review. *Proceedings of the Institution of Civil Engineers-Structures and Buildings*, 110(2), 186-203.

[5] Haidong, S. S. X. W. W., & Fei, L. K. Y. (2009). SSI effects on the dynamic behavior of structures: experimental study on a 1/4 scaled steel-frame building prototype. *China Civil Engineering Journal*.

[6] Idriss, I. M., & Akky, M. R. (1979). Primary variables influencing generation of earthquake motions by a deconvolution process. In *Structural mechanics in reactor technology. Transactions. Vol. K (a)*.

[7] Zeigler, D. J., Brunn, S. D., & Johnson Jr, J. H. (1981). Evacuation from a nuclear technological disaster. *Geographical review*, 1-16.

[8] Aden, M. A., Al-Attar, A. A., Hejazi, F., Dalili, M., & Ostovar, N. (2019, November). Effects of soil-structure interaction on base-isolated structures. In *IOP Conference Series: Earth and Environmental Science* (Vol. 357, No. 1, p. 012031). IOP Publishing.

[9] Alavi, E., & Alidoost, M. (2012). Soil-structure interaction effects on seismic behavior of base-isolated buildings. *Proc. 15th WCEE, Paper*, (4982).

[10] Sall, O. A., Fall, M., Berthaud, Y., Ba, M., & Ndiaye, M. (2014). Influence of the Soil-Structure Interaction in the behavior of mat foundation. *Open Journal of Civil Engineering*, *4*(01), 71.

[11] Boya, Y. (2014). *The Effect of Soil Structure Interaction on the Behavior of Base Isolated Structures* (Doctoral dissertation, Duke University).

[12] Pérez-Rocha, L. E., Avilés-López, J., & Tena-Colunga, A. (2021). Base isolation for mid-rise buildings in presence of soil-structure interaction. *Soil Dynamics and Earthquake Engineering*, *151*, 106980.

[13] Sachin, A. K., & Babu, B. J. (2020). Seismic Response of Fixed Base and Base Isolated RC Framed Building on Different Soil Conditions.

[14] Karabork, T., Deneme, I. O., & Bilgehan, R. P. (2014). A comparison of the effect of SSI on base isolation systems and fixed-base structures for soft soil. *Geomechanics and Engineering*, *7*(1), 87-103.

[15] Sravya, G. J., & Manchalwar, A. (2020). Comparison of Seismic isolation with isolator and Soil structure Interaction U-shaped metallic isolator and Soil structure Interaction. In *E3S Web of Conferences* (Vol. 184, p. 01097). EDP Sciences.

[16] Bandyopadhyay, S., Parulekar, Y. M., Sengupta, A., & Chattopadhyay, J. (2021, August). Structure soil structure interaction of conventional and base-isolated building subjected to real earthquake. In *Structures* (Vol. 32, pp. 474-493). Elsevier.

[17] Hassan, A., & Pal, S. (2018). Effect of soil condition on seismic response of isolated base buildings. *International Journal of Advanced Structural Engineering*, *10*(3), 249-261.

[18] Warn, G. P., & Ryan, K. L. (2012). A review of seismic isolation for buildings: historical development and research needs. *Buildings*, *2*(3), 300-325.

[19] Teodorescu, C. S., Diop, S., Politopoulos, I., & Benidir, M. (2013, June). A robust non-linear semi-active control for base seismically-isolated structures. In *21st Mediterranean Conference on Control and Automation* (pp. 545-550). IEEE.

[20] Cheng, F. Y. (2008). *Smart structures: innovative systems for seismic response control*. CRC press.

[21] Baratta, A., & Corbi, I. (2004). Optimal design of base-isolators in multi-storey buildings. *Computers & Structures*, *82*(23-26), 2199-2209.

[22] Wang, Y. P. (2002). Fundamentals of seismic base isolation. *International training programs for seismic design of building structures hosted by National Center of Research on Earthquake Engineering, Taiwan.*

[23] Chopra, A.R. (2001). "Dynamics of structures." Prentice-Hall, New Jersy, USA.

[24] M. Celebi, "Design of Seismic Isolated Structures: *From Theory to Practice," Earthq. Spectra*, vol. 16, no. 3, pp. 709–710, 2000.

[25] Raufaste, N. J. (1992). *Earthquake Resistant Construction Using Base Isolation: Survey Report on Framing of the Guidelines for Technological Development of Base-isolation Systems for Buildings*. NIST.

[26] Makris, N. (2019). Seismic isolation: Early history. *Earthquake Engineering & Structural Dynamics*, 48(2), 269-283.

[27] Robinson, W. H. (1996). Latest advances in seismic isolation. *Proc. XI WCEE*.

[28] Kawamura, S., Kitazawa, K., Hisano, M., & Nagashima, I. (1988, August). Study of a sliding-type base isolation system. System composition and element properties. In *Proceedings of 9th World Conference on Earthquake Engineering* (pp. 735-40).

[29] Zayas, V., Low, S. S. and Main, S. A. "The FPS earthquake resisting system, experimental report," *Report No. UCB/EERC-87/01, Earthquake Engineering Research Center, University of California, Berkeley, CA.*, June, (1987).

[30] Spencer, B. F., & Nagarajaiah, S. (2003). State of the art of structural control. *Journal of structural engineering*, *129*(7), 845-856.

[31] Matsagar VA, Jangid RS. "Influence of isolator characteristics on the response of base-isolated structures". *Engineering Structures*, 26(12), 1735-1749, 2004.

[32] Mishra, P., & Awchat, G. D. (2017). Lead Rubber Bearings as Base Isolating Devices for the Construction of Earthquake Resistant Structures-A Review. *SSRG International Journal of Civil Engineering (SSRG-IJCE)*, 4(7), 18-20.

[33] Bouc, R. (1967). Forced vibrations of mechanical systems with hysteresis. In *Proc. of the Fourth Conference on Non-linear Oscillations, Prague, 1967*.

[34] Wen, Y. K. (1976). Method for random vibration of hysteretic systems. *Journal of the engineering mechanics division*, *102*(2), 249-263.

[35] Naeim, F., & Kelly, J. M. (1999). *Design of seismic isolated structures: from theory to practice*. John Wiley & Sons.

[36] Hashash, Y.M.A., Phillipes, C. and Groholski, D. (2010). Recent Advances in Non-linear site response analysis, 5th International Conference on Recent Advances in Geotechnical Earthquake Engineering and Soil Dynamics, *San Diego*, California, 1-21.

[37] Kramer, S. L. (1996). Geotechnical earthquake engineering, Prentice Hall Upper Saddle River. *New Jersey*, 07458.

[38] Bolisetti, C. (2010). Numerical and physical simulations of soil-structure interaction *(Doctoral dissertation, MS Thesis, University at Buffalo, The State University of New York, Buffalo, New York).*

[39] Kanai, K. (1951). Relation between the nature of surface layer and the amplitude of earthquake motions. *Bulletin Earthquake Research Institute*.

[40] Idriss, I. M., & BOLTON SEED, H. (1967). Response of horizontal soil layers during earthquakes.

[41] Hashash, Y. M. A., Groholski, D. R., Phillips, C. A., Park, D., & Musgrove, M. (2011). DEEPSOIL 5.0, user Manual and Tutorial. *University of Illinois, Urbana, IL, USA*.

[42] Kondner, R. L. (1963). A hyperbolic stress-strain formulation for sands. In *Proc. 2 nd Pan Am. Conf. on Soil Mech. and Found. Eng., Brazil, 1963* (Vol. 1, pp. 289-324).

[43] Masing, G. "Eignespannungen und Verfestigung beim Messing." *Second International Congress on Applied Mechanics, Zurich, Switzerland*, 332-335.

[44] Darendeli, M. B. (2001). *Development of a new family of normalized modulus reduction and material damping curves*. The university of Texas at Austin.

[45] Konstantinidis, D., & Nikfar, F. (2015). Seismic response of sliding equipment and contents in base-isolated buildings subjected to broadband ground motions. *Earthquake engineering & structural dynamics*, *44*(6), 865-887.

Appendix

Base isolation numerical modeling by MATLAB

In this work, a SDOF on top of a LRB that is modeled as a Bouc-Wen element is used. Values of the Bouc-Wen model of the isolator are:

$\alpha = 0.1, \quad \beta = 0.1, \quad \gamma = 0.9, \quad n = 2$

α is the ratio of post-yield stiffness to elastic stiffness. The parameter n controls how sharp the transition from elastic to inelastic is. The parameters β and γ control the shape of the loops.

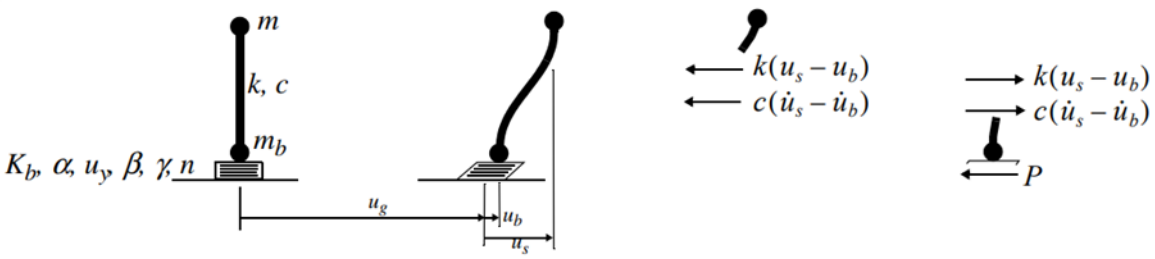

Figure 7 SDOF Structure on LRB [45]

Ordinary differential equations (ODEs) are the equation of motions. That means it only uses ordinary derivatives, not partial derivatives, and interest values are only functions of time. The fact is that ODEs are second order. The main concept we will employ comes from ODEs theory, which states that each n-order ODE can be described as a system of n first-order ODEs. In this work, the ODEs solver in MATLAB is recommended for solving the equation of motions.

$M\ddot{\upsilon}_s + k(\upsilon_s - \upsilon_b) = -m\ddot{\upsilon}_g$

$m_b \ddot{\upsilon}_b - k(\upsilon_s - \upsilon_b) + p = m_b \ddot{\upsilon}_g$

$p = \alpha k_e \upsilon(t) + (1 - \alpha) k_e \upsilon_y z(t)$

$m_b \ddot{\upsilon}_b + \alpha k_e \upsilon(t) + (1 - \alpha) k_e \upsilon_y z(t) - k(\upsilon_s - \upsilon_b) = m_b \ddot{\upsilon}_g$

$z(t)$ = Bouc Wen model

$\upsilon_y \dot{z} + \Upsilon|\acute{\upsilon}b|\ z\ |z^{n-1}| + \beta\ \acute{\upsilon}(t) - |z^n| - \acute{\upsilon}_b = 0$

Solution of the state-space equations of motion in MATLAB

$y = (y_1 \quad y_2 \quad y_3 \quad y_4 \quad y_5)^T = (\upsilon_s \quad \acute{\upsilon}_s \quad \upsilon_b \quad \acute{\upsilon}_b \quad z)^T$

$$\dot{y}(t =) \begin{pmatrix} y1 \\ y2 \\ y3 \\ y4 \\ y5 \end{pmatrix} = \begin{pmatrix} \acute{\upsilon}s \\ \ddot{\upsilon}s \\ \acute{\upsilon}b \\ \ddot{\upsilon}b \\ \dot{z} \end{pmatrix} = \begin{pmatrix} y2 \\ -\frac{1}{m} * k(y1 - y3) - \ddot{\upsilon}g \\ y4 \\ -\frac{1}{m}[\ \alpha\ \text{ke}\ y3 + (1 - \ \alpha)\text{ke}\ uy - k(y1 - y3) - \ddot{\upsilon}g \\ \frac{1}{uy}\ [-y4 - \Upsilon\ |y4|\ |y5^{n-1}| - \beta\ y4\ |y5^n| \end{pmatrix}$$

DEEPSOIL

In SA, soil properties are quite essential. Table 3 lists the material property of the soil. The dynamic characteristic of soil is taken from Bandyopadhyay et al. [16].

Table 6.1 Soil Parameters

Soil layer	Thickness (m)	Shear wave velocity (m/s)	Soils Density (kn/m^3)	Shear strain (m/s)	Poison's ratio
Layer one	30	350	20	245	0.1

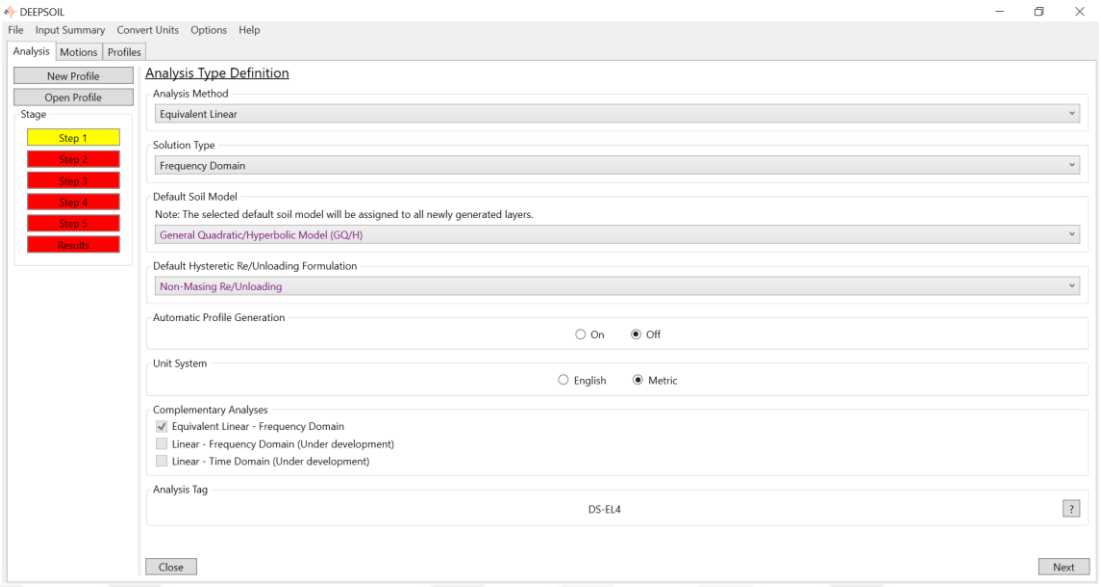

Figure 8 Soil Analysis Specification

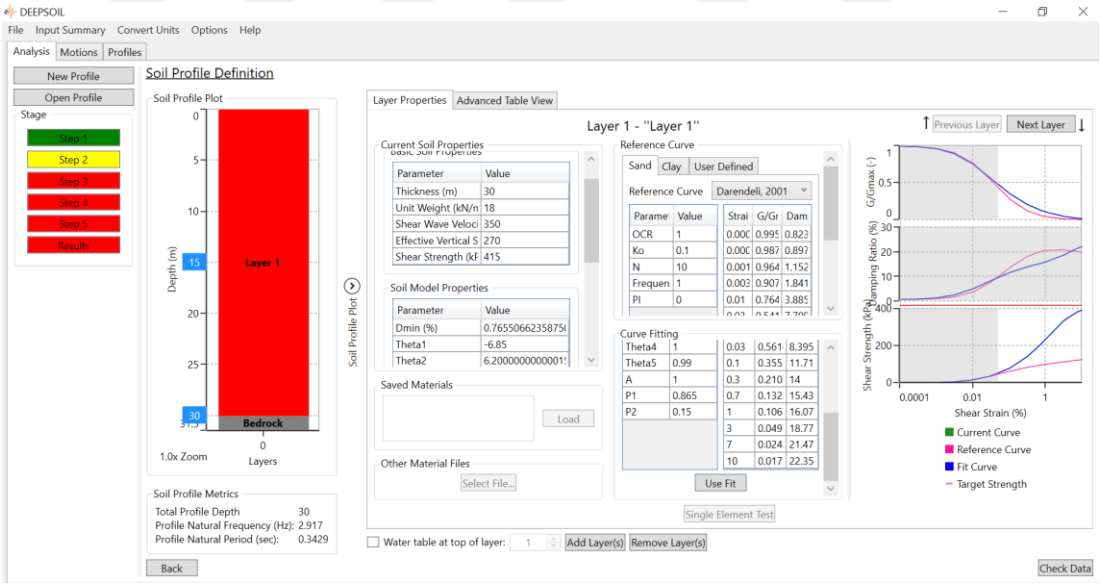

Figure 9 Parameters of Soil Analysis

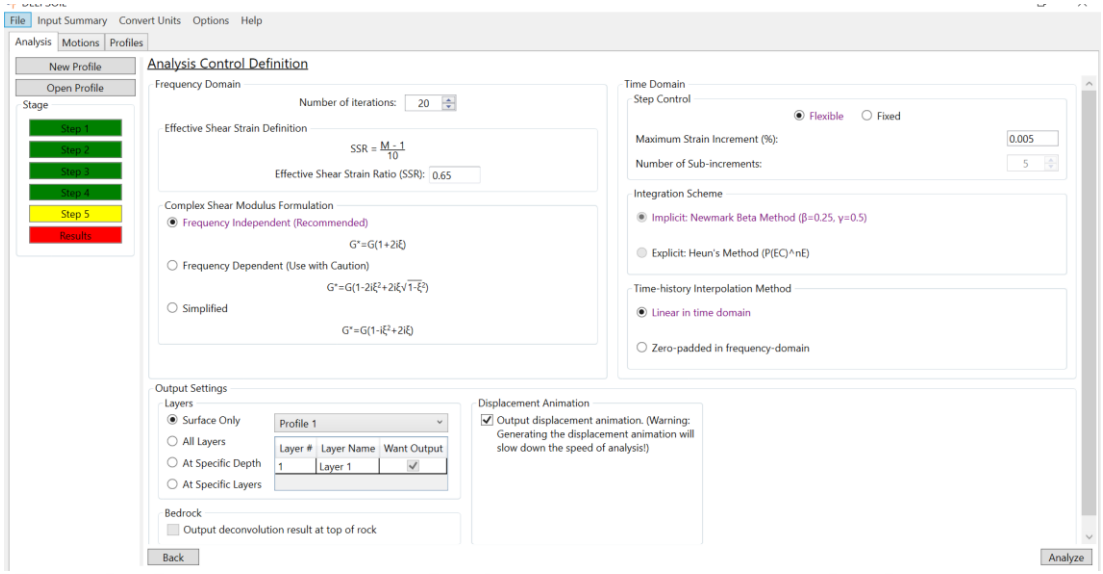

Figure 10 Soil Analysis

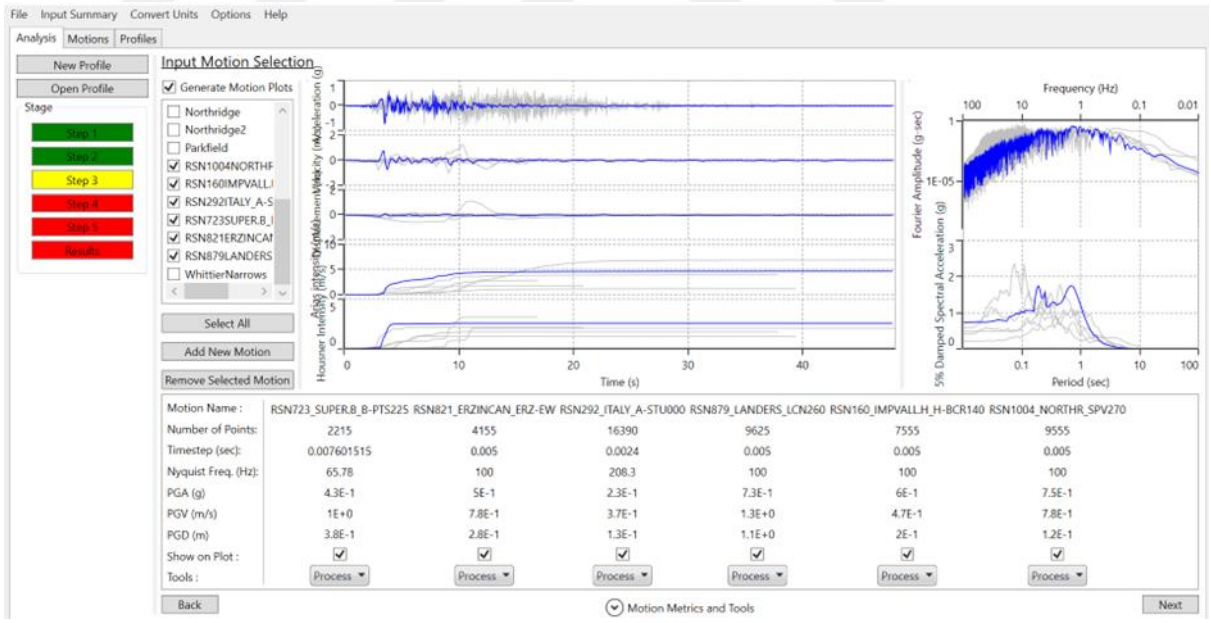

Figure 11 Description of Soil Analysis

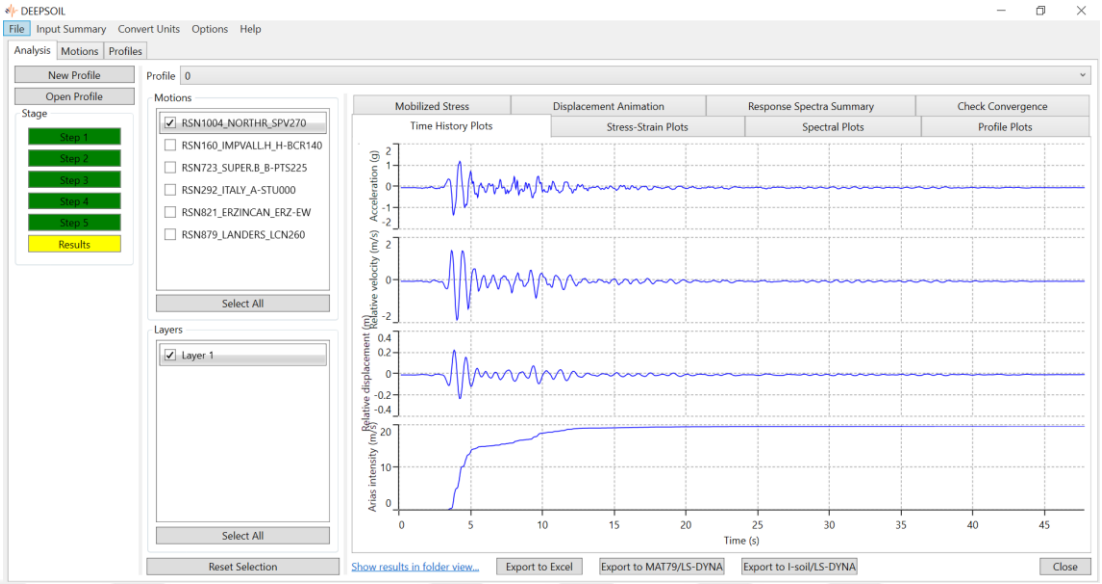

Figure 12 Result of Soil Analysis